

Migration of
radionuclides in
Boom Clay
PA model 'Clay'

OPERA-PU-NRG7212

Radioactive substances and ionizing radiation are used in medicine, industry, agriculture, research, education and electricity production. This generates radioactive waste. In the Netherlands, this waste is collected, treated and stored by COVRA (Centrale Organisatie Voor Radioactief Afval). After interim storage for a period of at least 100 years radioactive waste is intended for disposal. There is a world-wide scientific and technical consensus that geological disposal represents the safest long-term option for radioactive waste.

Geological disposal is emplacement of radioactive waste in deep underground formations. The goal of geological disposal is long-term isolation of radioactive waste from our living environment in order to avoid exposure of future generations to ionising radiation from the waste. OPERA (OnderzoeksProgramma Eindberging Radioactief Afval) is the Dutch research programme on geological disposal of radioactive waste.

Within OPERA, researchers of different organisations in different areas of expertise will cooperate on the initial, conditional Safety Cases for the host rocks Boom Clay and Zechstein rock salt. As the radioactive waste disposal process in the Netherlands is at an early, conceptual phase and the previous research programme has ended more than a decade ago, in OPERA a first preliminary or initial safety case will be developed to structure the research necessary for the eventual development of a repository in the Netherlands. The safety case is conditional since only the long-term safety of a generic repository will be assessed. OPERA is financed by the Dutch Ministry of Economic Affairs and the public limited liability company Electriciteits-Produktiemaatschappij Zuid-Nederland (EPZ) and coordinated by COVRA. Further details on OPERA and its outcomes can be accessed at www.covra.nl.

This report concerns a study conducted in the framework of OPERA. The conclusions and viewpoints presented in the report are those of the author(s). COVRA may draw modified conclusions, based on additional literature sources and expert opinions. A .pdf version of this document can be downloaded from www.covra.nl.

OPERA-PU-NRG7212

Title: Migration of radionuclides in Boom Clay, PA model 'Clay'

Authors: J.B. Grupa, J.C.L. Meeussen, E. Rosca-Bocancea (NRG),
D. Buhmann, E. Laggiard (GRS), A. F. B. Wildenborg (TNO)

Date of publication: 24 March 2017

Keywords: migration, Boom Clay, performance analysis

Summary	4
Samenvatting	4
1. Introduction	5
1.1. Background	5
1.2. Objectives.....	5
1.3. Realization	5
1.4. Explanation contents	5
2. Conceptual model for the Boom Clay PA model	6
2.1. OPERA safety assessment methodology.....	6
2.2. Compartment model for Boom Clay	6
2.2.1. Geological and geohydrological properties of the Boom Clay.....	7
2.2.2. Mineralogical and geochemical properties of the Boom Clay	8
2.2.3. Migration of species and radionuclides in the Boom Clay.....	9
2.3. Interface of the Boom Clay with adjacent compartments	10
2.3.1. Waste/EBS-clay interface	10
2.3.2. Clay-aquifer interface	11
3. Possible evolution of the host rock	13
3.1. Geological and hydrological evolution of the host rock.....	13
3.2. Brief outline of the normal evolution and altered evolution scenarios	14
4. Mathematical PA model for radionuclide migration in Boom Clay	16
4.1. Generic 1D nuclide diffusion model	16
4.2. Parameters values (Diffusion processes)	18
4.3. Linear model for reactive transport: the K_d approach	19
4.4. Simultaneous transport of nuclides as free aqueous ions and bound to colloids ..	22
4.5. Parameters values (Sorption processes)	27
4.6. Implementation in the PA model CLAY	29
4.7. Solubility limit.....	31
4.8. Effect of non-linear Freundlich adsorption.....	33
4.9. Approach used in PA model	34
5. Boom Clay model computer code, input data and parameters.....	35
5.1. The ORCHESTRA computer code	35
5.2. Required input	35
5.3. Required output.....	38
6. Benchmark ORCHESTRA vs. CLAYPOS.....	41
6.1. Benchmarking code	41
6.2. Benchmark case	42
6.3. Results of CLAYPOS calculations	44
6.4. Results of ORCHESTRA calculations	46
6.5. Comparison CLAYPOS and ORCHESTRA results.....	49
7. Conclusions and recommendations	53
8. References	54
Appendix 1 Diffusion accessible porosity.....	56
Appendix 2 Advection diffusion equation	59
Appendix 3 Diffusive versus advective transport.....	61

Summary

Theme of the present report is the transport of radionuclides from the repository through the host rock to the aquifer system. The host rock (Boom Clay) is the second model compartment succeeding the source (waste, container and EBS) and is followed by the aquifer system model.

Boom Clay is investigated as potential host rock for the geological disposal of radioactive waste due to its low permeability, its content of solid organic matter, its high cation exchange capacities (CEC) and high specific surface areas of the clay minerals. These characteristics, which are mainly defined by the clay minerals, further delay the slow diffusion of potentially released radionuclides.

The transport path has been modelled as one-dimensional. The numerical implementation has been tested both for a linear and a complex adsorption clay model with homogeneous properties (porosity, retardation). The calculations have been performed by the ORCHESTRA code. By benchmarking with the code CLAYPOS it is shown that ORCHESTRA is a suitable tool.

The presented results are able to explain the expected behaviour of the system, the Normal Evolution Scenario. For further scenarios, the same instruments can be used, if the transport path can be still modelled as one-dimensional. For all kind of calculations in the future, special emphasis should be given to radionuclide decay chains, because the combination of radioactive ingrowth and retardation (e.g. different K_d values of radionuclides in a chain) can strongly influence the results.

Samenvatting

Het onderwerp van dit rapport is het transport van radionucliden vanuit de opbergfaciliteit door het gastgesteente naar het aquifer-systeem. Het gastgesteente (Boomse klei) is het tweede model compartiment na de afvalcontainer/galerijstructuur en wordt gevolgd door het aquifer systeem model.

Boomse klei is onderzocht als potentieel gastgesteente voor een geologische opbergfaciliteit voor radioactief afval, vanwege zijn lage permeabiliteit, zijn gehalte aan vast organisch materiaal, zijn hoge kation-uitwisselingscapaciteit (CEC) en hoge specifieke oppervlak van de kleimineralen. Deze karakteristieken, die bepaald worden door de kleimineralen, vertragen de toch al langzame diffusie van eventuele vrijgezette radionucliden door deze geologische afzetting.

Het transport wordt gemodelleerd met een 1-dimensionaal model. Het rekenmodel is getest voor een kleimodel met lineaire adsorptie en een met complexer adsorptiegedrag, met homogene eigenschappen (porositeit, retardatie). Berekeningen zijn uitgevoerd met ORCHESTRA. Benchmarking met de CLAYPOS code laat zien dat ORCHESTRA een geschikte tool is.

De resultaten zijn consistent met het verwachte gedrag van het systeem, het normale evolutie scenario. Voor andere scenario's kan dezelfde tool ingezet worden, zolang het transportpad met een eendimensionaal model beschreven kan worden. Voor toekomstige berekeningen moet nadruk gegeven worden aan de radionuclide-vervalketens, omdat de combinatie van radioactieve ingroei en retardatie (bijv. verschillen in K_d waarden van radionucliden in een vervalketen) een sterke invloed op de resultaten kan hebben.

1. Introduction

1.1. Background

The five-year research programme for the geological disposal of radioactive waste - OPERA - started on 7 July 2011 with an open invitation for research proposals. In these proposals, research was proposed for the tasks described in the OPERA Research Plan (Verhoef & Schröder, Research Plan, 2011).

1.2. Objectives

This report describes the execution and results of the research proposed for Task 7.2.1 with the following title in the Research Plan: *PA model for radionuclide migration in Boom Clay*.

The main objective of this task is to set up a PA modelling code for calculating the migration of radionuclides from the waste packages through the Boom Clay host rock to the enclosing geosphere. The proposed modelling and calculation approach is based on the findings of WP 6.1.2 (*Modelling of sorption processes*), WP 6.1.3 (*Modelling of diffusion processes*), WP 6.1.4 (*Mobility and presence of colloidal particles*), WP 4.2 (*Geohydrological boundary conditions for the near-field*), and WP 5.2 (*Properties, evolution and interactions of the Boom Clay*) and served as direct input to Task 7.2.2 (*PA model for radionuclide migration in the rock formation surrounding the host rock*) and Task 7.2.4 (*Integrated modelling environment for safety assessment*).

1.3. Realization

This report has been compiled by NRG, TNO and GRS. TNO has compiled information on the geological structure of the overburden. The calculations by the computer codes ORCHESTRA and CLAYPOS have been performed by NRG and GRS, respectively.

1.4. Explanation contents

Chapters 2 and 3 provide the description of the conceptual PA compartment model for reactive transport of radionuclides through the Boom Clay. Chapter 4 describes the mathematical model, and Chapters 5 and 6 provide the description of the computer code and the testing of the implementation of the mathematical model. The conclusions and recommendations are summarized in Chapter 7.

2. Conceptual model for the Boom Clay PA model

The conceptual PA model applied in OPERA represents the region between the disposed waste and potential receptors (i.e. humans) in our environment. The region between the waste and the receptor is conceptually divided into compartments: (1) the waste matrix and the engineered barriers, (2) the clay host rock, (3) the overburden (including any aquifer systems) that surrounds the clay host rock, and (4) the biosphere (including potential receptors).

The basic premise is that the radionuclides have to move from the waste through each of these compartments to reach the receptors in the biosphere. The various scenarios differ in the processes that drive the radionuclide migration through each of the compartments and/or the pathways available for radionuclide transport through the compartments.

2.1. OPERA safety assessment methodology

The present report describes the formulation and implementation of the assessment model for the host rock (Boom Clay) compartment as defined in step four of the recommended safety assessment methodology for the OPERA project, see (Grupa J. , 2014, pp. 11, 14).

Step 4, formulation and implementation of Assessment Models requires:

1. A conceptual model. The conceptual model provides a description of the components of the system and the interactions between these components.
2. A mathematical model, which is a mathematical representation of the features and processes included in the conceptual model.
3. A computer code, which is a software implementation of the mathematical model that facilitates performance of the assessment calculations.

The present chapter and Chapter 3 provide the description of the conceptual model. Chapter 4 describes the mathematical model, and Chapters 5 and 6 include the description of the computer code and the testing of the implementation of the mathematical model.

2.2. Compartment model for Boom Clay

The conceptual model for the performance analysis of the total disposal system developed in OPERA represents the region between the disposed waste and potential receptors (i.e. humans) in our environment. This region is conceptually divided into compartments, which are in line with the multi-barrier system approach described in (Verhoef & Schröder, Research Plan, 2011), p.8.

The following compartments are defined in the PA model for OPERA:

- The Waste-EBS compartment, consisting of the waste form, the waste package and the repository building & affected materials (or enclosing engineered barrier system);
- The Host Rock (Boom Clay);
- The Overburden (note that the rock formations below the host rock are included in this compartment, too)
- The Biosphere.

The evolution of the repository can be described by the following steps (Figure 2-1):

- 1) The waste packages are emplaced in disposal galleries. The lining and the plugs are intact, and therefore the inside of the disposal gallery is initially dry.
- 2) The gallery internals will become saturated with water, probably within some decades. For LILW, the waste may start to leach (slowly) relatively soon after

closure. For the HLW, the canister and overpack will fail after some thousands of years, and soluble species will start to leach from the HLW matrix. Eventually, all sections of the disposal facility will be saturated with pore water intruding from the clay.

- 3) Due to the water content of the clay rock, soluble radionuclides that will eventually be released from the repository will migrate through water in the pore network of the clay. Even without relevant water flow, after some thousands of years, radionuclides will have migrated a significant distance into the host rock. Mobile nuclides will have migrated a few tens of meters, less immobile nuclides not more than one meter. After a few tens of thousands years the mobile nuclides will have reached the aquifer system. Less mobile nuclides will reach the aquifer (much) later.

Most of the radioactive material will never reach the aquifer, since it is either virtually immobile or has will have decayed during the slow migration through the clay.

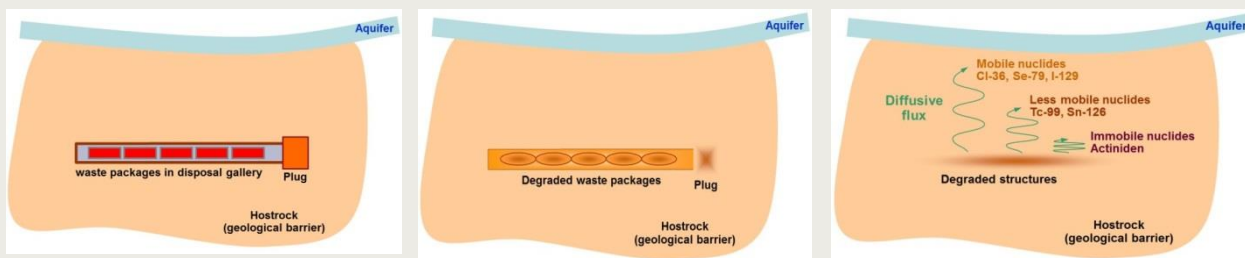


Figure 2-1 Migration of nuclides through the clay host rock

The work carried out in OPERA WP4 (*Geology and geohydrology*) supports the assumption that there are sites in The Netherlands where Boom Clay can provide in the safety functions R2 (No water flow near the waste), R3 (Slow transport to aquifer) and I2 (Stable conditions for the EBS).

For such sites, the work in WP5.2 (*Properties, evolution and interactions of the Boom Clay*) and WP6.1 (*Radionuclide migration in Boom Clay*) shows that with high probability nuclides can only migrate very slowly, driven by molecular diffusion in the clay pore water. Moreover, many radionuclides are sorbed on the clay minerals or on immobile organic matter present in the clay layer, retarding the migration even more.

Some less likely scenarios have been identified in which faster migration may occur. These scenarios are the Abandonment Scenario, Poor Sealing Scenario, Undetected Fault Scenario and Human Intrusion Scenarios (Grupa, Hart, & Wildenborg, 2017). For some less likely events it is not clear what the consequences may be: e.g. excessive gas generation or a criticality event. Indicative results for the performance of the disposal system in these circumstances can often be obtained by changing parameter values in the calculations, e.g. using a smaller thickness of the clay layer, reducing the absorption factors, or by assuming advective transport through the clay layer.

2.2.1. Geological and geohydrological properties of the Boom Clay

The geological and geohydrological properties of the Boom clay were investigated within WP4 and reported in (Vis & Verweij, 2014). According to that study, in some areas the top of the Rupel Clay Member (Boom Clay) is located deeper than 400 m below the mean sea level and the member is over 100 m thick. Two main areas meeting these criteria can be identified: the Roer Valley Graben in Noord-Brabant and Limburg and the eastern part of the Zuiderzee Low, underneath the Veluwe area. In the rest of the country, several small

zones meeting the criteria can be identified. Fault systems cutting through the member are known to be more numerous in the Roer Valley Graben. This is unknown for the Zuiderzee Low. Fault properties (horizontal and vertical offset, geohydrological properties, connectivity) are unknown but will have to be assessed with respect to the Safety Functions.

In the areas where the Rupel Clay Member is over 100 m thick and its top is located deeper than -400 m m.s.l. limited grain-size data are available. In the north of the country several small zones meeting the depth-thickness criteria have been identified. The median grain size (D50) in that well shows low values between 8 and 10 μm , justifying the interpretation as a medium silt. In that well there appears to be no grain-size coarsening towards top and base of the member. Wells in the southwest (B41G0024 and B46C0478) show an average D50 grain size which is similar to that of wells in the north (see below). Well B58G0192 (southeast Netherlands), however, contains the coarser deposits, with D50 grain-size values reaching up to 166 μm . This can be explained by its position near a palaeo-coastline.

NIRAS/ONDRAF [ONDRAF/NIRAS 2013, p.85] reports that grain size variations in the Boom Clay are generally small, ranging from clayey silt to silty clay. They also report local deviations caused by eustacy (global sea level change), and also by local tectonics and climate change during deposition.

Table 2-1 Grain size variations in the Boom Clay reported in (Vis & Verweij, 2014)

<i>Size range</i>	<i>Aggregate name (Wentworth Class)</i>	<i>Other names</i>
62.5-125 μm	Very fine sand	
4-62.5 μm	Silt	Mud
1-4 μm	Clay	Mud
1-1000 nm	Colloid	Mud

In line with the lithofacies distribution, the calculated permeability of the Rupel Clay Member is lowest in the north of the Netherlands and higher and more variable in the south and southeast. Generally the permeability decreases with increasing depth for the same lithology. At 500 m depth the calculated vertical permeabilities range from $1\text{E-}19$ to $1\text{E-}18 \text{ m}^2$. This is consistent with the range reported by NIRAS (ONDRAF/NIRAS, 2013), p.93.

In Appendix 3 it is shown that for these conditions the diffusive vertical transport dominates over the advective vertical transport through the clay.

2.2.2. Mineralogical and geochemical properties of the Boom Clay

The main mineralogical and geochemical properties of the Boom Clay reported in (Koenen & Griffioen, 2014) are summarized below.

Clay rocks are investigated as potential host rock for the geological disposal of radioactive waste due to their low permeability, high cation exchange capacities (CEC) and high specific surface areas of the clay minerals. These characteristics, which are mainly defined by the clay minerals, influence the diffusion of potentially released radionuclides through the sediment. Unfortunately, a stratigraphic sequence is not (yet) available for the Dutch Boom Clay.

The high CEC is mainly due to the presence of smectite. The results for this task of the OPERA program show that the mineralogical clay content of the Boom Clay is much larger in the northern part of the Netherlands than in the south. The smectite content in the XRD clay fraction analysis reaches the highest values (>50 wt%) for the samples in the north.

The potential effects of pyrite oxidation and of thermal stress on kerogen (solid organic matter) is relevant for heat generating radioactive waste storage in Dutch Boom Clay, regardless of the location of the repository, since heat may cause the kerogen to release components, like hydrocarbons, ketones and alkanolic acids (and complexated radioactive elements if they are released from the waste during the thermal phase).

Overall, there is a clear division between the northern and the southern part of the Netherlands.

- The northern part is much more clay-rich, is fine grained and relatively homogeneous with depth. The samples have a relatively high carbonate content.
- In the south-western part of the country the Boom Clay is more silty. Here, the upper and/or lower parts of the Boom Clay are coarser grained and contain more quartz and feldspar. The middle parts of the Boom Clay are finer grained and more clay-rich with an occasional sandy layer. (Note that in that area the depth of the Boom Clay is less than 400 m.)
- In the south-eastern part, the Boom Clay is in generally more sandy and carbonate-rich than in the south-western part.

Septarian concretions have not yet been identified and analysed in the Netherlands. These septarian layers might influence fluid flow at the reservoir scale, forming more or less continuous, horizontal high permeability layers within the low permeable Boom Clay member. Their presence can be expected, at least in the south of the Netherlands.

In Belgium, since 2001 the National Commission of Stratigraphy has modified the limit between the Belsele-Waas and Terhagen members and has introduced the Boeretang Member. The Boom Clay now consists of the Boeretang Member, Putte Member, Terhagen Member, and the Belsele-Waas Member. The layered structure of the Boom Clay contains easily recognisable features such as the pink horizon in the Terhagen Member, the boundary between the grey clay of the Terhagen Member and the black clay of the Putte Member (position URL), the Double Band in the Putte Member and about 20 septaria levels (carbonate concretions) (ONDRAF/NIRAS, 2013), p.84-85.

The main components of the Boom Clay in Belgium are:

Quarz	20% - 70%
Illite/muscovite	5% - 40%
Smectite / illite smectite	5% - 40%
Kaolinite	2% - 14%
Solid Natural Organic Matter	1% - 5%
Others	1% - 30%

Septaria levels are not taken into account (ONDRAF/NIRAS, 2013), p.87-88.

About 10% of the Natural Organic Matter is dissolved in the pore water (DOM) and has the potential to increase the mobility of certain radioactive elements (ONDRAF/NIRAS, 2013), p.111.

2.2.3. Migration of species and radionuclides in the Boom Clay

The geological, geohydrological, mineralogical and geochemical studies in OPERA have shown that there are potential sites in the Netherlands where the Boom Clay may have the required properties for serving as a host rock. The properties relevant for the conceptual model for the PA are:

- the top of the clay layer is at 500 m depth or deeper
- the clay layer is 100 m thick or thicker
- the permeability is low, advective transport plays no role
- the clay has a high adsorption capacity

- the clay provides a stable environment for the facility

Under these conditions it can be assumed that the migration of radionuclides released from the waste and the EBS is dominated by diffusion, and adsorption plays an important role for most radionuclides.

The geometry of the facility and the clay layer is vertically small (100 m) in comparison with the horizontal dimensions (thousands of meters). Therefore the general migration direction through the clay is vertical. However, near to the EBS, the migration direction also has a horizontal component. From each of the canisters radionuclides are migrating, initially in a spherical pattern. At some distance these patterns will merge to a one dimensional pattern, where concentration gradients in horizontal directions disappear, as illustrated in Figure 2-2.

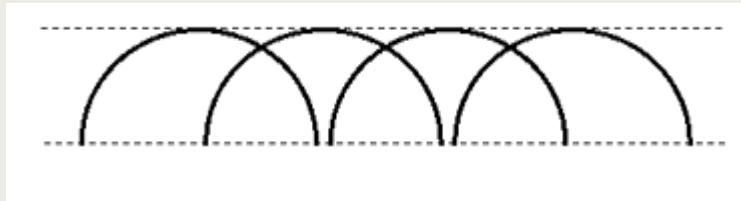


Figure 2-2 Circular concentration patterns merge into a flat concentration profile

For the migration calculation, the plane of canisters in the clay layer can be replaced by a sheet of waste. In that geometry, no horizontal concentration gradients occur, and the mathematical equations become one dimensional.

It should also be noted that the transport distance in the sheet-like geometry is shorter than in the true repository geometry, because the latter part of the transport path does exhibit a horizontal component. In effect, the calculated migration fluxes are slightly conservative, although the calculated concentration near the sheet is lower than the actual concentrations near the canisters in a true 3D-representation.

2.3. Interface of the Boom Clay with adjacent compartments

The host rock interfaces with the adjacent compartments Waste-EBC and overlying formations (aquifer or geosphere). This section describes the conceptual model for these interfaces.

2.3.1. Waste/EBS-clay interface

The waste compartment contains the waste, the waste package and the EBS. Open spaces and pores are filled with water (or gas). The water is modelled as a homogeneous mixing tank.

$$C(t) = \frac{A(t)}{V} = \frac{A_d(t) - A_a(t) - A_{out}(t)}{V}$$

$C(t)$ concentration of radionuclides in water at time t

V volume of the water

$A(t)$ amount of radionuclides in the water at time t

$A_d(t)$ amount of radionuclides dissolved from the waste matrix up to time t

$A_a(t)$ amount of radionuclides absorbed to EBS materials at time t

$A_{out}(t)$ amount of radionuclides that has migrated into the clay up to time t

The flux from the waste compartment to diffusion dominated Boom Clay layer is assumed to be determined by diffusion, which is the main transport mechanism in Boom clay [Meeussen, 2014b; Section 3.4]. The diffusion through the interface is controlled by the concentration gradient and average porosity and tortuosity of the adjacent compartments.

As pointed out in the previous section, at some distance from the EBS the concentration profile and fluxes can be closely approached by one-dimensional diffusion, i.e. as if the source is a flat layer of waste and EBS materials. In that geometry, the diffusion profile and fluxes are only driven by the amount of material dissolved in the 'source layer'.

This amount M is:

$$M(t) = A_d(t) - A_a(t)$$

2.3.2. Clay-aquifer interface

Radionuclides from the repository migrate through the clay and enter the aquifer at about 500 m depth, and these radionuclides reach the surface through the aquifer system, where they can enter the biosphere.

On a conceptual level of the model, the interface between the clay and the aquifer at 500 m depth is regarded as a sharp transition from almost impermeable clay to a permeable, sandy aquifer. Actually, however, the transition is more gradual: at the top and the bottom of the clay layer more and more sand sheets are observed, and the character of the soil gradually changes from low permeable, highly adsorbing clay to permeable, low adsorbing sandy soils (Figure 2-3).

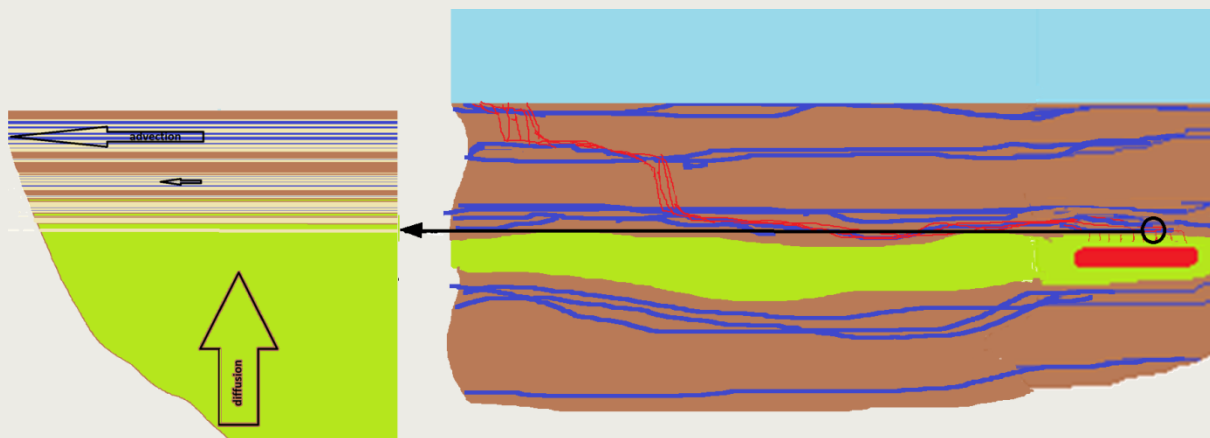


Figure 2-3 Schematic overview of the clay-aquifer interface

The radionuclide diffusion in the clay is driven by the concentration gradient. The aquifer acts as a sink in the interface: due to the flow of water in the sandy layers in the aquifer, the water in the aquifer is continuously refreshed, and radionuclides are removed from the interface, causing a relatively low concentration in the aquifer water at the interface. Sandy layers exhibiting a low water velocity are less efficient as a sink as to layers with a higher water velocity. Sandy layers with an extremely low water speed (deeper in the clay, not connected to a percolating network) don't act as a sink at all.

The diffusive migration through the clay can be conservatively calculated by assuming that the radionuclide concentration in the aquifer water is zero. This allows the clay model to calculate the rate at which the radionuclides transfer from the clay to the aquifer. The average concentration of radionuclides in the aquifer water can be calculated by dividing the radionuclides transfer rate by the water flow rate of the aquifer. Since the flow rate in the deep aquifer is very low, this approach may be overly conservative.

The precise approach is to balance the rate at which the radionuclides leave the clay formation and the rate at which radionuclides are removed from the interface area:

- The rate at which the radionuclides leave the clay formation depend on the (apparent) diffusion constant in the clay, the concentration gradient in the clay, and the length and width of the area where the radionuclides leave the clay and enter the aquifer. The latter are roughly equal to the size of the repository, i.e. a few square kilometres.
- The rate at which radionuclides are removed from the interface area depends on the water velocity in the aquifer, and the width and height of that part of aquifer through which the nuclides are transported. This width is about equal to the width of the repository, the height is a few meters.

3. Possible evolution of the host rock

This section deals with the evolution of the far-field of the host rock, which is not or negligibly influenced by the presence of the repository and the heat producing high-level radioactive waste. It is assumed that the top of the host rock, i.e. the Boom Clay, is at depth of 500 m or more.

3.1. Geological and hydrological evolution of the host rock

Geological and hydrological process at the earth's surface and in the earth's interior can be split in two main groups with different origins: exogenous processes which are climate related and strongly driven by the radiation of the sun and endogenous tectonic processes which are related to the dynamics of the earth's mantle and crust. An extensive description of both groups of processes is given in (Veen & Dario, 2015).

Climate induced processes

On a time scale of 100 ka the earth experiences significant changes in solar irradiation due to quasi-periodic variations in the position of the earth relative to the sun (astronomical or Milankovitch Theory). These changes led to the regular glaciation of mid-latitude continents in the past 800 ka. The Netherlands was twice partly covered by ice, in the Elsterian and the Saalian glaciation.

A major cooling during a future glacial period may influence the temperature at depths of 500 m or more. Although glaciation has major consequences for the overburden, see (Verweij, Nelskamp, Valstar, & Govaerts, 2016), permafrost is not expected to reach depths of 500 m as the maximum depth for the NL conditions is 270 m according to simulations done by SCK, (Veen & Dario, 2015), Section 5.1.

Due to glacial loading the clay host rock will be deformed which leads to the expulsion of consolidation water. This release will enhance the transport of radionuclides through the host rock into shallower ground. Simulation work in the TRACTOR project (Wildenborg, et al., 2000) showed that under current conditions dispersive transport contributes to 0.08% and under glacial conditions to 0.2% without ice loading and 14% with ice loading. The episodic occurrence of ice loading with an assumed duration of 20,000 years and a periodicity of 100,000 years increases the radionuclide mass flux at the interface between the clay barrier and the upper aquifer. The maximum value of the radionuclide advective mass flux is temporarily 2 to 9 times the advective mass flux in the reference scenario (current climate conditions). This is still less than the diffusive mass flux.

The stress increase in the subsurface (both horizontal and vertical stresses and the shear stress) as a consequence of glaciation, intensifies seismic activity and activates fault movement. This happens in particular during the phase of rapid deglaciation (Veen & Dario, 2015), Section 4.2. Glaciotectonic structural deformation can occur to a depth of 500 m only in the most extreme case (Veen & Dario, 2015). The Saalian glaciation in the Netherlands lead to structural deformation of up to 150 m below current sea-level, see www.dinoloket.nl - REGISII v2.1: gestuwde afzettingen, complexe eenheid. It is not expected that the host rock at a depth of 500 m or more will be directly influenced by glaciotectonic structural deformation.

In very exceptional cases subglacial erosion may reach depths of 400 m (Groot, Berg, Dijke, Jansen, & Veldkamp, 1993) which would not directly reach the assumed depth of the top at 500 m. The production of large volumes of meltwater at the basis of the ice sheet which is recharged to the subsurface aquifers, may influence radionuclide transport in the host rock. Further work is reported in (Valstar & Goorden, 2016).

If the recharged meltwater is oxygenated this may lead to chemical changes in the Boom Clay to depths of about 10 m with an exposure duration of about 1 ka. The sulphate concentration might increase due to the oxidation of sulphide but the pH is not expected to drop below 7 in the presence of sufficient carbonate (Jansen & Griffioen, 2014).

A large temperature drop could lead to the formation of methane hydrates (Veen & Dario, 2015). Methane Hydrates cannot form at depths of 500 m or more due to the high temperatures at these depths (LLNL, 1999). Research on temperature evolution is reported in (Verweij, Nelskamp, Valstar, & Govaerts, 2016).

Tectonic processes

New faults only form in response to changes in the pattern of tectonic stress; such changes appear to occur very slowly and can be discarded for the considered future time span of 1 Ma (Veen & Dario, 2015), p.72.

Sedimentary loading, e.g. during prograding sedimentation of delta wedges or gas pressure build-up in the subsurface, may lead to the formation of (sub-)vertical chimney or pipe structures which act as conduits for expelled fluids (Veen & Dario, 2015).

Geochemical processes

No large geochemical changes are expected to happen in the Boom Clay during the next 1 million years if the system is not disturbed by natural or anthropogenic factors (Jansen & Griffioen, 2014). The clay mineralogy will not be changed by diagenetic processes since pressure, temperature and pH are not expected to change relevantly in the next 1 million years.

Organic matter will hardly degrade as it is subjected to constant reducing conditions which stabilized the current state of the organic matter. No destabilizing factors like oxidizing conditions are present and chemical gradients are absent. In such circumstances alterations induced by microbes are considered to be limited.

3.2. Brief outline of the normal evolution and altered evolution scenarios

The normal evolution scenario (NES) and altered evolution scenarios for the OPERA Research Programme have been described in (Grupa, Hart, & Wildenberg, 2017). The host rock properties are constant in all assessment cases of the NES.

Several altered evolutions scenarios were identified in (Grupa, Hart, & Wildenberg, 2017). These are:

- Abandonment Scenario: the host rock is bypassed by non-sealed shafts and access galleries. This condition can obviously only be initiated on the short term before the repository will be closed.
- Poor Sealing Scenario: the host rock is bypassed by poorly sealed shafts, access and/or disposal galleries.
- Anthropogenic greenhouse scenario: increased risk of flooding of the repository as a consequence of the rising sea-level in the next hundreds of years. As a result, brackish water may infiltrate in the shallow subsurface or in the repository in case it has not yet been closed.
- Fault Scenario: the host rock is bypassed by a non-observed fault (re-activated) transecting the repository and the overburden (or 'chimney') which acts as a conduit for mobilized radionuclides.

- Intensified glaciation scenario: an ice sheet is covering the repository area and leads to deep subglacial erosion to 400 m at a maximum or a permafrost layer with a thickness of 300 m is present. In case of glaciation, meltwater will be recharged to the subsurface aquifers and consolidation water will be expelled from the Boom Clay.
- Human Intrusion and Human Action Scenarios: the host rock will be bypassed by drilling for resource exploitation like hydrocarbons, geothermal energy or potable water.

In addition to the identified scenarios several more cases, so-called “What-if cases”, have been identified which are not yet included in an altered evolution scenario. These what-if cases are:

- EEC1 Excessive Early Container Failure: the host rock is intact.
- EGC1 Excessive Gas assessment case: gas pressure increases within the host rock.
- EFD1 Fast and radical dissolution of the waste: the host rock is intact.
- ECC1 Criticality event: heat release may affect the host rock.
- EHP1 Excessive heat production: thermal stress and chemical alteration may affect the host rock.

4. Mathematical PA model for radionuclide migration in Boom Clay

In this chapter the reactive transport equations are derived that can be used for the Normal Evolution Scenario and most of the Altered Evolution Scenarios. The transport equations consist of a differential equation to describe the transport and equations to include the boundary conditions.

These differential equations can be solved numerically. In the OPERA research program the open source computer code ORCHESTRA (Meeussen, ORCHESTRA: An object-oriented framework for implementing chemical equilibrium models, 2003) is used for:

1. determining the adsorption behaviour of Boom Clay (Schröder & Meeussen, Final report on radionuclide sorption in Boom Clay, 2017) in terms of linear adsorption coefficients K_d , and,
2. performing the nuclide migration calculations for the OPERA disposal system (Verhoef, Neeft, Grupa, & Poley, 2011)

The actual implementation of the Boom clay properties and the disposal system properties in ORCHESTRA are here referred to as the NRG-CLAY-tool and NRG-PA-tool, respectively.

Mathematical Model	ORCHESTRA implementation	Verification
OPERA-PU-NRG6123: mechanistic adsorption model for the calculation of correlated sets of K_{d_diss} and K_{d_DOC} for all elements	NRG-CLAY-tool v2016 (Schröder & Meeussen, Final report on radionuclide sorption in Boom Clay, 2017)	benchmark with K_d ranges provided by SCK·CEN
OPERA-PU-NRG7212 (this report): 1D diffusive transport with linear adsorption	NRG-PA-tool v2017 (see Chapter 5)	benchmark with ClayPos (GRS) (see Chapter 6)

Sections 4.1, 4.2 and 4.3 describe the mathematical representation of the diffusion process in a one-dimensional geometry (this is generalised to three-dimensional geometry, see Appendix 2). This mathematical model is a common pollutant transport model that has already been used in the '70s and '80s in the safety studies in e.g. Belgium and France.

Section 4.4 and 4.5 describe a much less common extension to the transport model, representing simultaneous transport of dissolved radionuclides and radionuclides bound to dissolved organic material (DOC). This extension to the model gives a good understanding of the two transport processes, allows a better understanding of the impact of DOC, and also it removes some conservatism that is an implication of the more common approach to this: choosing only one transport mode and using conservative parameter values.

Section 4.6 describes how the mathematical model is implemented in the NRG-PA-tool. Section 4.7 describes the implementation of a solubility limit in the NRG-PA-tool. Section 4.8 gives an illustration of the impact of a more realistic non-linear adsorption model and how this is covered by the linear adsorption model.

4.1. Generic 1D nuclide diffusion model

As pointed out in Section 2.2.3, in the Normal Evolution Scenario, the migration can be approximated by a one dimensional process, where all waste canisters are mathematically

represented by a sheet in the middle of the clay layer and no horizontal concentration gradient exists.

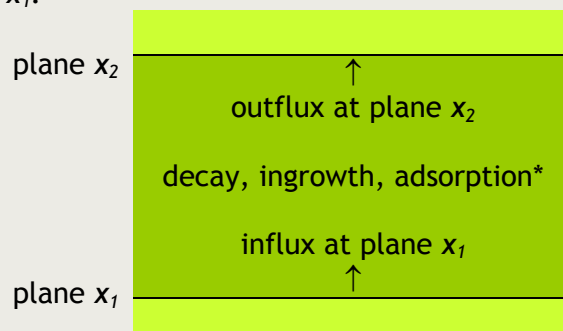
In that geometry, a vertical directed diffusive flux of a dissolved species (such as a radionuclide) through a horizontal plane can be calculated using Fick's first law, see also (ONDRAF/NIRAS, 2001, p. 11.3.8.2.1):

$$J = -\eta_{da} A G D_{aq} \frac{dC}{dx} \quad \text{Eq. 4-1}$$

with:

J diffusive mass flux [mol/s] through a horizontal area A [m²],
 D_{aq} diffusion coefficient or diffusivity of the solute in free water or 'free-solution' diffusion coefficient (in absence of porous medium) [m²/s],
 η_{da} diffusion accessible porosity [-],
 G geometry factor accounting for the pore structure (i.e. tortuosity, constrictivity),
 C aqueous phase concentration of the solute [mol/m³],
 x distance in the direction of transport [m].

The diffusion equation can be obtained by setting up a mass balance between two planes at x_1 and x_2 , where $x_2 > x_1$.



N.B. The PA model is restricted to decay, ingrowth, and adsorption, but in general also other processes such as precipitation can be introduced here.

where the change of the amount of radionuclides (Δn in mol) during a time Δt is:

$$\text{influx at plane } x_1: \quad \Delta n_{x_1} = -\eta_{da} A G D_{aq} \left. \frac{\delta C}{\delta x} \right|_{x_1} \Delta t$$

$$\text{outflux at plane } x_2: \quad \Delta n_{x_2} = \eta_{da} A G D_{aq} \left. \frac{\delta C}{\delta x} \right|_{x_2} \Delta t$$

$$\text{decay in volume } A(x_2 - x_1) \quad \Delta n_{decay} = -\lambda n \Delta t$$

$$\text{ingrowth from parents } p \quad \Delta n_{ingrowth} = \sum_p Y_p \lambda_p n_p \Delta t$$

Eq. 4-2

So:

$$\Delta n_{total} = -\eta_{da} A G D_{aq} \left. \frac{\delta C}{\delta x} \right|_{x_1} \Delta t + \eta_{da} A G D_{aq} \left. \frac{\delta C}{\delta x} \right|_{x_2} \Delta t - \lambda n \Delta t + \sum_p Y_p \lambda_p n_p \Delta t \quad \text{Eq. 4-3}$$

The above equation is the transport equation that is numerically solved by the NRG-PA-tool (Section 5.1), where an Euler explicit scheme is used to estimate the concentration gradients at the planes x_1 and x_2 .

Dividing all terms by the volume $A(x_2-x_1)$ and by ∂t , and substituting (x_2-x_1) by ∂x , the equation becomes:

$$\frac{\partial B_{total}}{\partial t} = \eta_{da} G D_{aq} \frac{\partial^2 C}{\partial x^2} - \lambda B_{total} + \sum_p Y_p \lambda_p B_{p,total} \quad \text{Eq. 4-4}$$

where:

- B_{total} total concentration (including the adsorbed fraction) in a small volume at location x at time t [mol/m³],
- C aqueous phase concentration of the solute [mol/m³],
- η_{da} diffusion accessible porosity [-],
- G geometry factor accounting for the pore structure (i.e. tortuosity, constrictivity),
- D_{aq} diffusion coefficient of the nuclide in free water [m²/s],
- λ radioactive decay constant [s⁻¹],
- λ_p radioactive decay constant of the parent nuclides p [s⁻¹],
- Y_p yield (fraction of nuclides p that decay to the nuclide represented by C),
- $B_{p,total}$ total concentration of the parent in a small volume at location x at time t [mol/m³].

If a species is non-reactive (not sorbed), and if the diffusion accessible porosity η_{da} equals the total porosity η , $B_{total} = \eta \cdot C = \eta_{i,da} \cdot C$, Eq. 4-4 can be divided by η (or η_{da}) and takes the common form of the diffusion equation (and $B_{p,total} = 0$ for all p):

$$\frac{\partial C}{\partial t} = G D_{aq} \frac{\partial^2 C}{\partial x^2} - \lambda C \quad \text{Eq. 4-5}$$

Experiments with tritiated water have shown that this equation gives a good description of the migration in clay: (ONDRAF/NIRAS, 2001), Section 11.3.8.4.1.

4.2. Parameters values (Diffusion processes)

The subject of OPERA Task 6.1.3 was the diffusion of radionuclides in Boom Clay and its model representation (Meeussen, et al., 2017). The overall diffusion is determined by a combination of physical and chemical processes and interactions, Task 6.1.3 focused on the physical aspects of diffusion processes. That task resulted in ranges of values for the diffusion accessible porosity and the pore diffusion coefficient for each nuclide.

When combining transport properties with the chemistry (adsorption), an elaboration of the understanding of "porosity" is needed. (Shackelford & Moore, 2013) distinguish the following types of porosities:

- | | |
|--|--|
| total porosity (η) | total volume of water (in a unit of a saturated porous medium) |
| diffusion accessible porosity (η_{da}) | volume of the water in the pores that is accessible by diffusion for a given species |
| effective or through-diffusion porosity (η_i) | volume of the water that is accessible by diffusion and is interconnected |

The use of an effective porosity in lieu of a diffusion accessible porosity takes into account the possibility that there may be pores that are not interconnected and, therefore,

represent dead ends (i.e. dead-end pores), such that only a fraction of the pore space may be available for mass transport.

For many materials the effective or through-diffusion porosity is almost equal to the diffusion accessible porosity. In practise, in literature the term diffusion accessible porosity is often used in those instances where, following the more strict definitions of (Shackelford & Moore, 2013), the term effective or through-diffusion porosity should be used.

However for fractured rock, highly compacted bentonite buffers and smectitic based geologic formations, (Shackelford & Moore, 2013) report a considerable amount of dead-end pores in the form of immobile liquid fraction ("bound water") in the interparticle and interlayer pore spaces within each clay particle. Boom clay contains a considerable amount of smectites (10% - 20%), therefore it must be expected that for Boom clay $\eta_i < \eta_{da}$.

This leads to the following equality between the data in (Meeussen, et al., 2017) and the equations derived in the previous section:

$$\eta_i D_{pore,i} = \eta_{da} G D_{aq} \quad \text{Eq. 4-6}$$

- i index referring to one of the nuclides that will be released from the waste
- η_i effective or through-diffusion porosity for the nuclide i [-], varying from 0.05 to 0.4; addressed as diffusion accessible porosity in (Meeussen, et al., 2017), Table 6-9 (note that $\eta_i \leq \eta_{da}$.)
- $D_{pore,i}$ pore diffusion coefficient, varying from 5.7E-12 to 8.5E-9 m²/s ((Meeussen, et al., 2017), Table 6-9)

For nuclide i the diffusion equation becomes:

$$\frac{\partial B_{total,i}}{\partial t} = \eta_i D_{pore,i} \frac{\partial^2 C_i}{\partial x^2} - \lambda_i B_{total,i} + \sum_p Y_p \lambda_p B_{p,total} \quad \text{Eq. 4-7}$$

Note that the diffusion characteristics apply to nuclides dissolved in the pore water as well as nuclides that are sorbed to dissolved organic matter (DOM); in the latter case the values for $D_{pore, coll}$, η_{coll} are used.

4.3. Linear model for reactive transport: the K_d approach

Adsorption is characterized by the amount of nuclides adsorbed on a given mass of solid material and the concentration of the radionuclide in the water surrounding this mass of solid material.

Consider a volume V of saturated porous material. A key parameter is the amount of a species that is adsorbed to the porous matrix material. In general, this amount depends on the mass of the absorbing material in the volume V , the adsorption processes, the chemical composition (pH, Eh, etc.), the presence of other species - precipitated or in solution in the pore water, and the chemical reactions that can occur in this mixture.

The principal adsorption behaviour of Boom Clay can be estimated experimentally in so-called *batch experiments*, by creating a solution that is chemically similar to the pore water, by dissolving a given amount of the species in this solution, and by adding a given mass of Boom Clay to the solution. A fraction of the species will be adsorbed by the clay and the dissolved concentration decreases.

The result of the experiment is recorded as the distribution coefficient K_d [m^3/kg]:

$$n_{i,adsorbed} = K_d M_s C_i \quad \text{Eq. 4-8}$$

M_s	mass (kg) of the solid
$n_{i,adsorbed}$	the amount (moles) of nuclide i adsorbed to the mass M_s
K_d	distribution coefficient (m^3/kg)
C_i	concentration (moles/ m^3) of nuclide i in the pore water

The K_d is defined as the amount of species i sorbed per unit mass of substrate (M_s the mass of the dry clay) divided by the dissolved amount of species i .

Distribution coefficients can also be calculated using geochemical modelling codes and thermodynamic databases for chemical equilibria. The main advantage of such calculated distribution coefficients is that the model calculations provide insight into the dependence of the K_d values for variation or changes in the chemical conditions of the system. This not only helps to translate experimental (lab) results to field scale but also enables to translate results from e.g. Belgian to Dutch underground conditions.

Evaluation of the accuracy of such theoretical model calculations for complex materials, such as natural clays, can be done by comparing results with experimental results.

Although sorption processes are generally non-linear, for elements at low concentrations, such as relevant for radionuclides, the assumption of linear adsorption behaviour as used in the K_d approach can be adequate for a PA.

Assuming a constant K_d is called the K_d approach.

The K_d approach is applicable in combination with following assumptions:

- the reactions are reversible,
- the solid and liquid phase are in equilibrium,
- the equilibrium concentrations can be described by linear equations,
- only water saturated porous media are considered.

Assuming a linear K_d model gives a relation between $B_{i,total}$ and C_i , as follows. Consider a volume V of saturated porous material:

the mass of the solid is: $M_s = \rho_{dry} V$

the amount (moles) of nuclide i adsorbed is proportional to the amount (mass) of absorbing material (M_s): $n_{i,adsorbed}$

the volume of the water is: $V_{water} = \eta V$

the amount (moles) of nuclide i dissolved is: $n_{i,dissolved} = C_i \eta V$

with η (total) porosity [1].

So $B_{total,i}$ (in mol/m^3) is:

$$B_{total,i} = \frac{n_{i,adsorbed}(M_s)}{V} + C_i \eta \quad \text{Eq. 4-9}$$

Substituting $n_{i,adsorbed}$ by $K_d M_s C_i$ gives:

$$B_{total,i} = \frac{K_d M_s}{V} C_i + C_i \eta = \frac{K_d \rho_{dry} V}{V} C_i + C_i \eta = K_d \rho_{dry} C_i + C_i \eta \quad \text{Eq. 4-10}$$

Note that the amount of species that is dissolved is taken to be $V \eta C_i$, where η is the porosity of the clay (for Boom Clay the porosity ranges from 29% to 43%). This implies that it is assumed that all pores are accessible for the dissolved species, even though experimental results have suggested that the through-diffusion porosity (η_i) is smaller than the total clay porosity for some dissolved species. Since the diffusion accessible porosity, as defined by (Shackelford & Moore, 2013), may be larger than the through-diffusion porosity for smectitic clays such as Boom Clay, this implies that the diffusion accessible porosity η_{da} is close to the total porosity η . Alternative assumptions are described in Appendix 1.

If not all pores are available for diffusive transport, but all pores are included in the chemistry, the equation above leads to:

$$B_{total,i} = K_d \rho_{dry} C_i + C_i \eta = \eta \left(1 + \frac{K_d \rho_{dry}}{\eta} \right) C_i \quad \text{Eq. 4-11}$$

Substitute $B_{total,i}$ into Eq. 4-7 results in:

$$\frac{\partial C_i}{\partial t} = \frac{\eta_i}{\eta} \frac{D_{pore,i}}{\left(1 + \frac{K_d \rho_{dry}}{\eta} \right)} \frac{\partial^2 C_i}{\partial x^2} - \lambda_i C_i + \sum_p \frac{Y_{p,i} \lambda_{p,i} B_{p,i,total}}{\eta \left(1 + \frac{K_d \rho_{dry}}{\eta} \right)} \quad \text{Eq. 4-12}$$

In this equation the chemical retention factor R_i or retardation factor for nuclide i is defined as:

$$R_i = 1 + \frac{K_d \rho_{dry}}{\eta} \quad \text{Eq. 4-13}$$

where:

- R_i the retention factor [1]
- K_d distribution coefficient (m^3/kg)
- ρ_{dry} is the dry density (kg/m^3) of the clay ($= M_s/V$)

Substituting $R_i = 1 + \frac{K_d \rho_{dry}}{\eta}$ and $B_{p,i,total} = \eta R_{p,i} C_{p,i}$ in the equation gives the diffusion equation:

$$\frac{\partial C_i}{\partial t} = \frac{\eta_i D_{pore,i}}{\eta R_i} \frac{\partial^2 C_i}{\partial x^2} - \lambda_i C_i + \sum_p Y_{p,i} \lambda_{p,i} \frac{R_{p,i}}{R_i} C_{p,i} \quad \text{Eq. 4-14}$$

where:

- C_i aqueous phase concentration in the diffusion accessible pores of nuclide i [mol/m^3],
- $D_{pore,i}$ pore diffusion coefficient of nuclide i [m^2/s],
- η_i through-diffusion porosity [1] for the species bearing nuclide i
- η (total) porosity [1],
- R_i (chemical) retention or retardation factor of nuclide i [-],
- λ_i radioactive decay constant of nuclide i [s^{-1}],
- $\lambda_{p,i}$ radioactive decay constant of the parent nuclide of nuclide i [s^{-1}],
- $Y_{p,i}$ yield of nuclide p decaying to nuclide i
- $R_{p,i}$ (chemical) retention or retardation factor of the parent nuclide of nuclide i [-],
- $C_{p,i}$ aqueous phase concentration of the parent nuclide of nuclide i [mol/m^3].

Note that for $\eta_i < \eta$ the apparent diffusion decreases by a factor η_i/η in addition to the decrease caused by adsorption as expressed in R_i . Since a factor η_i/η is caused by the assumed pore geometry (i.e. dead end pores), and not by the chemistry, this factor is not included in R_i .

Apparent diffusion

The diffusion properties can be derived from the adsorption behaviour of species, as shown above. In addition, SCK.CEN has measured the apparent diffusion of various species in diffusion and percolation experiments. The apparent diffusion coefficient (Shackelford & Moore, 2013, p. eq (23)) is introduced in terms of the diffusion equation, such that, without decay and ingrowth:

$$\frac{\partial C_i}{\partial t} = D_{app} \frac{\partial^2 C_i}{\partial x^2} \quad \text{Eq. 4-15}$$

By determining the change of concentration profiles in diffusion and percolation experiments, the value of D_{app} can be determined.

For the PA model 'clay' D_{app} is:

$$D_{app} = \frac{\eta_i D_{pore,i}}{\eta R_i} = \frac{\eta_i}{\eta} \left(\frac{D_{pore,i}}{1 + \frac{K_d \rho_{dry}}{\eta}} \right) \quad \text{Eq. 4-16}$$

Note that (ONDRAF/NIRAS, 2001, p. 11.3.8.2.1) uses a slightly different terminology:

$$D_{app} = \frac{D_{aq}}{RR_f} = \frac{GD_{aq}}{R} = \frac{D_{pore,i}}{R} \quad \text{(ONDRAF/NIRAS, 2001, p. 11.3.8.2.1)}$$

where:

$$R = 1 + \frac{K_d \rho_{dry}}{\eta_{i,da}} \quad \text{(ONDRAF/NIRAS, 2001, p. 11.3.8.4.5),}$$

Although D_{app} is not explicitly defined in (ONDRAF/NIRAS, 2001), it is reasonable to assume that it has the same meaning as expressed in Eq. 4-15. However, if $R > 1$, (ONDRAF/NIRAS, 2001) postulates that $\eta_{i,da} = \eta$, which removes the difference with respect to R . A more detailed discussion is given in Appendix 1.

4.4. Simultaneous transport of nuclides as free aqueous ions and bound to colloids

For some nuclides a significant fraction is bound to organic matter, either solid or as colloids, and a small fraction is present as free aqueous species. Examples of these nuclides are isotopes of Ra, Sr, Cs, Ni and U (see Figure 4-12 in (Schröder & Meeussen, Final report on radionuclide sorption in Boom Clay, 2017)). In this case it may be unclear which dissolved phase (free aqueous species or bound to dissolved organic materials, DOC) dominates the transport: the larger amount of nuclides bound to DOC migrate slower than the smaller amount of the same nuclide dissolved as free aqueous species.

The common approach is to choose for each nuclide the dominant transport process, and use slightly conservative parameter values to cover the contribution of the secondary transport process.

The mathematical model set out in Sections 4.1, 4.2 and 4.3 allows a (less common) extension in order to represent simultaneous transport of dissolved radionuclides and radionuclides bound to dissolved organic material (DOC). This extension to the model provides a good understanding of the contribution of both transport processes, allows a better understanding of the impact of DOC, and also it removes some conservatism inherent in the more common approach to this: choosing only one transport mode and using conservative parameter values.

The PA-model allows treatment of transport of nuclides as free aqueous ions and bounded to colloids simultaneously, as follows.

Diffusive transport

Some nuclides simultaneously migrate as free ions and/or bound to DOC. Diffusion of the nuclides that are dissolved as free ions is described by a through-diffusion porosity η_i and the product of G and D , resulting in:

$$J_{free} = -A\eta_i D_{pore,free} \frac{\partial C_{free}}{\partial x} \quad \text{Eq. 4-17}$$

where:

- J_{free} diffusive mass flux [mol/s] of the aqueous nuclide through a horizontal area A [m²],
- C_{free} aqueous phase concentration of the radionuclides not bound to DOC in the soluble phase [mol/m³],
- $D_{pore,free}$ pore diffusion coefficient of aqueous nuclide [m²/s],
- η_i through-diffusion porosity [1] for the species bearing nuclide i

Diffusion of the nuclides that are dissolved, but bound to DOC, is described as:

$$J_{DOC} = -A\eta_{DOC} D_{pore,DOC} \frac{\partial C_{DOC}}{\partial x} \quad \text{Eq. 4-18}$$

where:

- J_{DOC} diffusive mass flux [mol/s] of the DOC-bound nuclide through a horizontal area A [m²],
- C_{DOC} concentration of the radionuclides not to DOC in the soluble phase [mol/m³],
- $D_{pore,DOC}$ pore diffusion coefficient of DOC particles [m²/s],
- η_{DOC} through-diffusion porosity [1] for DOC particles

And the total diffusive flux is:

$$J = J_{DOC} + J_{free} \quad \text{Eq. 4-19}$$

To ease the next mathematical operations, the aqueous concentrations of the free ions and the DOC (i.e. the concentration in the pore water) are converted into total concentrations in the saturated porous medium (i.e. the amount of dissolved ions in a unit volume containing pore water and the porous material). Note that this "spatial" concentration has the same units as the concentration in water (both mol/m³). To make a distinction, the symbol B is used for the spatial concentration.

Note again that the amount of material that is dissolved is taken to be $V \eta C_i$, where η is the porosity of the clay (for Boom clay the porosity ranges from 29% to 43%). So:

$$C_{free} = \frac{B_{free}}{\eta} \quad \text{Eq. 4-20}$$

and:

$$C_{DOC} = \frac{B_{DOC}}{\eta} \quad \text{Eq. 4-21}$$

gives for the diffusive flux:

$$J = -A \frac{\eta_i}{\eta} D_{pore,free} \frac{\partial B_{free}}{\partial x} - A \frac{\eta_{DOC}}{\eta} D_{pore,DOC} \frac{\partial B_{DOC}}{\partial x} \quad \text{Eq. 4-22}$$

In a one-dimensional geometry, the volume V can be defined as the volume between $x = x_1$ and $x = x_2$, where we choose $x_1 < x_2$. The increase of the amount of nuclides n_{total} in volume V is (over a short time interval Δt is equal to the influx at x_1 minus the outflux at x_2):

$$\begin{aligned} \Delta n_{total} &= \Delta B_{total} A (x_2 - x_1) \\ &= (J(x_1) - J(x_2)) \Delta t + \left(-\lambda_i B_{total} + \sum_p Y_{p,i} \lambda_{p,i} B_{p,i} \right) A (x_2 - x_1) \Delta t \end{aligned} \quad \text{Eq. 4-23}$$

which can be rewritten as:

$$\frac{\Delta B_{total}}{\Delta t} = \frac{(J(x_1) - J(x_2))}{A(x_2 - x_1)} = -\frac{1}{A} \frac{(J(x_2) - J(x_1))}{(x_2 - x_1)} - \lambda_i B_{total} + \sum_p Y_{p,i} \lambda_{p,i} B_{p,i} \quad \text{Eq. 4-24}$$

If $\Delta t \rightarrow 0$ and $x_1 \rightarrow x_2$:

$$\frac{\partial B_{total}}{\partial t} = -\frac{1}{A} \frac{\partial J}{\partial x} - \lambda_i B_{total} + \sum_p Y_{p,i} \lambda_{p,i} B_{p,i} \quad \text{Eq. 4-25}$$

Substituting J gives the transport equation:

$$\begin{aligned} \frac{\partial B_{total}}{\partial t} &= \frac{\eta_{DOC}}{\eta} D_{pore,DOC} \frac{\partial^2 B_{DOC}}{\partial x^2} + \frac{\eta_i}{\eta} D_{pore,free} \frac{\partial^2 B_{free}}{\partial x^2} - \lambda_i B_{total} \\ &\quad + \sum_p Y_{p,i} \lambda_{p,i} B_{p,i} \end{aligned} \quad \text{Eq. 4-26}$$

Chemical equilibrium

If all adsorption processes are linear with the concentration and are reversible, the following relations hold:

$$n_{absorbed} = K_{d,free} M_s C_{free} \quad \text{Eq. 4-27}$$

and:

$$n_{absorbed} = K_{d,DOC} M_s C_{DOC} \quad \text{Eq. 4-28}$$

where:

$n_{adsorbed}$ amount (moles or Bq) of nuclides adsorbed to a mass M in the (pore) water
 $K_{d,free}$ distribution factor for free ions (m^3/kg)
 $K_{d,DOC}$ distribution factor for nuclides bounded tot DOC (m^3/kg)

M_s	mass of the adsorbing material (kg)
C_{free}	concentration (Bq/m ³ or kg/m ³) of free ions in the (pore) water
C_{DOC}	concentration (Bq/m ³ or kg/m ³) of nuclides bound to DOC in the pore water

In terms of the spatial concentrations B , this gives:

$$\begin{aligned}
 B_{free} &= \eta C_{free} \\
 B_{DOC} &= \eta C_{DOC} \\
 B_{absorbed} &= \frac{n_{absorbed}}{V} \\
 B_{total} &= B_{absorbed} + B_{free} + B_{DOC}
 \end{aligned}
 \tag{Eq. 4-29}$$

where:

B_{total}	total nuclide concentration per volume (adsorbed to the clay, dissolved and adsorbed to DOC)
$B_{adsorbed}$	spatial concentration of adsorbed nuclides (mol/m ³)
$n_{adsorbed}$	amount of nuclides adsorbed to the clay in volume V (mol)
η	total porosity of the clay (29% - 43%)
V	volume (m ³) of the saturated clay

Because of the chemistry, all concentrations (B_{total} , C_{free} , C_{DOC} , etc.) are proportional with constant factors for all places x and times t . E.g. if only free ions would diffuse into a volume of saturated clay, the linear adsorption chemistry will instantaneously restore the chemical balance between adsorbed, free ions and DOC bounded nuclides in that volume of clay.

The following chemical equilibrium concentrations hold for all times t and all places x in the clay:

$$B_{total} = \left(1 + \frac{K_{d,DOC}\rho_{dry}}{\eta} + \frac{K_{d,DOC}}{K_{d,free}} \right) B_{DOC} = \left(1 + \frac{K_{d,free}\rho_{dry}}{\eta} + \frac{K_{d,free}}{K_{d,DOC}} \right) B_{free}
 \tag{Eq. 4-30}$$

Using this to substitute B_{DOC} and B_{free} by B_{total} in the transport equation, gives:

$$\begin{aligned}
 \frac{\partial B_{total}}{\partial t} &= \left(\frac{\frac{\eta_{DOC}}{\eta} D_{pore,DOC}}{1 + \frac{K_{d,DOC}\rho_{dry}}{\eta} + \frac{K_{d,DOC}}{K_{d,free}}} + \frac{\frac{\eta_i}{\eta} D_{pore,free}}{1 + \frac{K_{d,free}\rho_{dry}}{\eta} + \frac{K_{d,free}}{K_{d,DOC}}} \right) \frac{\partial^2 B_{total}}{\partial x^2} \\
 &\quad - \lambda_i B_{total} + \sum_p Y_p \lambda_p B_{p,total}
 \end{aligned}
 \tag{Eq. 4-31}$$

The apparent diffusion coefficient is:

$$D_{app} = \frac{\frac{\eta_{DOC}}{\eta} D_{pore,DOC}}{1 + \frac{K_{d,DOC}\rho_{dry}}{\eta} + \frac{K_{d,DOC}}{K_{d,free}}} + \frac{\frac{\eta_i}{\eta} D_{pore,free}}{1 + \frac{K_{d,free}\rho_{dry}}{\eta} + \frac{K_{d,free}}{K_{d,DOC}}}
 \tag{Eq. 4-32}$$

Note that C_{free} and C_{DOC} are proportional to B_{total} , so the diffusion equation for these quantities is equal. Ignoring decay and ingrowth:

$$\begin{aligned}\frac{\partial B_{total}}{\partial t} &= D_{app} \frac{\partial^2 B_{total}}{\partial x^2} \\ \frac{\partial C_{free}}{\partial t} &= D_{app} \frac{\partial^2 C_{free}}{\partial x^2} \\ \frac{\partial C_{DOC}}{\partial t} &= D_{app} \frac{\partial^2 C_{DOC}}{\partial x^2}\end{aligned}\tag{Eq. 4-33}$$

Implementation in the PA model clay

These equations can be rewritten in the more common terms introduced in Sections 4.1 and 4.3 by introducing the concentration C : C is the concentration of the pore water of the dissolved nuclide, both as a free species and bounded to DOC:

$$C = C_{DOC} + C_{free}\tag{Eq. 4-34}$$

Note that also C must comply to the diffusion equation (ignoring decay and ingrowth):

$$\frac{\partial C}{\partial t} = D_{app} \frac{\partial^2 C}{\partial x^2}$$

This allows the introduction of K_d , R , and a new parameter f_{DOC} :

$$\begin{aligned}n_{adsorbed} &= K_d M_s C \\ R &= 1 + \frac{K_d \rho_{dry}}{\eta} \\ f_{DOC} &= \frac{C_{DOC}}{C}\end{aligned}\tag{Eq. 4-35}$$

Note that by using f_{DOC} , the diffusive transport is:

$$J = J_{free} + J_{DOC} = -A \left((1 - f_{DOC}) \eta_i D_{pore,i} + f_{DOC} \eta_{DOC} D_{pore,DOC} \right) \frac{\delta C}{\delta x}$$

The K_d can be related to $K_{d,DOC}$ and $K_{d,free}$ using the following steps:

$$\begin{aligned}n_{adsorbed} &= K_d M_s C = K_d M_s (C_{DOC} + C_{free}) = \\ &= K_d \left(\frac{K_{d,DOC} M_s C_{DOC}}{k_{d,DOC}} + \frac{K_{d,free} M_s C_{free}}{k_{d,free}} \right) = \\ &= n_{adsorbed} \left(\frac{K_d}{K_{d,DOC}} + \frac{K_d}{K_{d,free}} \right)\end{aligned}\tag{Eq. 4-36}$$

So:

$$\frac{K_d}{K_{d,DOC}} + \frac{K_d}{K_{d,free}} = 1\tag{Eq. 4-37}$$

which implies:

$$K_d = \frac{K_{d,DOC}K_{d,free}}{K_{d,DOC} + K_{d,free}} \quad \text{Eq. 4-38}$$

This is identical to Eq. 4-2 in (Schröder & Meeussen, Final report on radionuclide sorption in Boom Clay, 2017).

f_{DOC} relates to $K_{d,DOC}$ and $K_{d,free}$ as follows:

$$f_{DOC} = \frac{C_{DOC}}{C_{DOC} + C_{free}} \quad \text{Eq. 4-39}$$

Use Eq. 4-27 and Eq. 4-28:

$$n_{absorbed} = K_{d,free}M_sC_{free} = K_{d,DOC}M_sC_{DOC}$$

so:

$$f_{DOC} = \frac{K_{d,DOC}^{-1}}{K_{d,DOC}^{-1} + K_{d,free}^{-1}} \quad \text{Eq. 4-40}$$

In terms of R_{DOC} and R_{free} , this is as defined in (Schröder & Meeussen, Reference database with sorption properties, 2017):

$$R_{DOC} = 1 + \frac{k_{d,DOC}\rho_{dry}}{\eta} \quad \text{Eq. 4-41}$$

and:

$$R_{free} = 1 + \frac{k_{d,free}\rho_{dry}}{\eta} \quad \text{Eq. 4-42}$$

such that:

$$\frac{k_{d,DOC}}{k_{d,free}} = \frac{R_{DOC} - 1}{R_{free} - 1} \quad \text{Eq. 4-43}$$

This allows to rewrite K_d in terms of R :

$$R = 1 + \frac{(R_{DOC} - 1)(R_{free} - 1)}{R_{DOC} + R_{free} - 2} \quad \text{Eq. 4-44}$$

and:

$$f_{DOC} = \frac{\frac{1}{R_{DOC} - 1}}{\frac{1}{R_{DOC} - 1} + \frac{1}{R_{free} - 1}} \quad \text{Eq. 4-45}$$

4.5. Parameters values (Sorption processes)

The subject of OPERA Task 6.1.2 was the chemical interactions of nuclides with complexing ions in pore water and adsorbing surfaces in the solid and colloidal phases. So, the outcome of that Task is the expected distribution of nuclides over various chemical forms under Boom Clay conditions. Because these various forms differ in mobility (solid, colloidal, aqueous) this distribution is a determining factor describing the overall mobility of nuclides in Boom Clay.

The K_d values listed in (Schröder & Meeussen, Reference database with sorption properties, 2017) vary from 0 to 8'200 l/kg, i.e. from 0 to 8 m³/kg. Using central estimates for the bulk wet density (2025 kg/m³) and the clay porosity (36%) the retardation factors vary from 1 to 40'000.

In (Schröder & Meeussen, Final report on radionuclide sorption in Boom Clay, 2017), K_d values for a broad range of chemical conditions for the Boom clay have been determined using the NRG-Clay-tool implementation of ORCHESTRA. Since these calculations do not include a transport calculation, these calculations are computationally cheap, and a large number of calculations could be performed.

At present, the best characterisation of the Boom Clay still is expressed as a broad range of chemical conditions, because:

- for some thermodynamic properties of the Boom Clay there is actual little data and,
- the clay properties are location (or site) dependent, and,
- the location of a future repository is presently unknown, and,
- even if the location is known, spatial variability of the clay properties on the 1 - 1000 m scale, in combination with the experimental difficulty of determining precise values for the chemical parameters, the clay still will have to be characterised by ranges of chemical conditions.

To evaluate the adsorption, given this uncertainty in the chemical conditions, a very large number of thermodynamic calculations were performed by sweeping over the various parameters representing the chemical condition of the clay (Schröder & Meeussen, Final report on radionuclide sorption in Boom Clay, 2017). Each calculation results in a "point- K_d value" (i.e. only valid for that set of chemical conditions and concentrations). For each species the point- K_d values were converted to R values (using Eq. 4-13) and presented in scatterplots. From the percentiles in these plots the range of R (or K_d) values was derived that can be used in the linear- K_d model, where, using the range of K_d values in the linear- K_d model, will cover all point- K_d values found. Figure 4-4 illustrates this process for Tc and Sr.

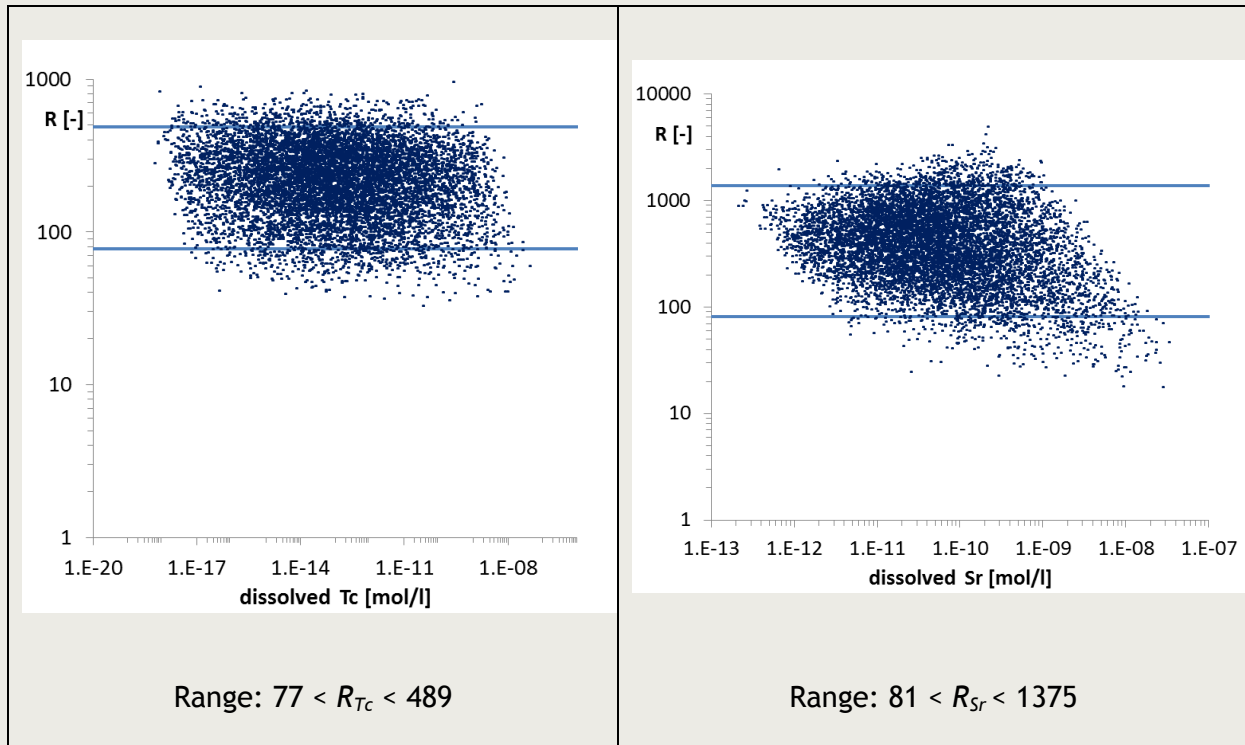


Figure 4-4 Determination of the range of R values of Cs and U

From the example figures it follows that for technetium the bounding R s for the linear K_d model are $R = 77$ at the low end and $R = 489$ at the high end, for strontium 81 resp. 1375. For conservative PA calculations the low-end values of R must be used.

The R and K_d values provide a very instructive intermediate result, since its impact on the PA can be easily understood qualitatively: a larger K_d means more adsorption, and slower transport, and, eventually, lower doses in the biosphere. E.g., sensitivity studies on the impact of chemical conditions on the K_d value can be directly interpreted for the PA without performing PA calculations.

4.6. Implementation in the PA model CLAY

The PA model for clay as implemented in ORCHESTRA uses a Finite Volume method for calculating the transport and concentrations over time. Finite volume methods use piecewise constant approximation spaces (grid elements). This yields exact conservation statements. The volume integral is converted to a surface integral and the entire physics is specified in terms of fluxes in those surface integrals (see also Appendix 2).

For the NRG-PA-tool implementation in ORCHESTRA, the integral (addressed as the *test function* in the Finite Volume method) is:

$$\Delta n_{total} = A \left((1 - f_{DOC}) \eta_i D_{pore,i} + f_{DOC} \eta_{DOC} D_{pore,DOC} \right) \left(\frac{\delta C}{\delta x} \Big|_{x_2} - \frac{\delta C}{\delta x} \Big|_{x_1} \right) \partial t + -\lambda n_{total} \partial t + \sum_p Y_{p,i} \lambda_{p,i} n_{p,i} \partial t \quad \text{Eq. 4-46}$$

where:

$$C = \frac{n_{total}}{\eta RA(x_2 - x_1)}$$

The NRG-PA-tool solves the integral with an Euler explicit scheme.

As described in the previous paragraphs, the combined set of parameters available in the Reference database with sorption parameters (OPERA M6.1.2.1.2), the mechanistic model to calculate K_d values and distribution fractions f_{DOC} (OPERA M6.1.2.3), and the Reference database with diffusion parameters (OPERA M6.1.3.2) provide the required information to supply the OPERA PA model with the required input data for diffusion of radionuclides through the Boom Clay compartment. The results of Task 6.1.3 (Presence, mobility and reactivity of colloids) are integrated in both reference databases.

Test of the implementation of the PA model in the NRG-PA-tool

For one-dimensional diffusion of a flat plane nuclide source in the centre ($x=0$) of an infinite clay medium, the diffusion equation (Eq. 4-14) can be solved analytically for those nuclides that have no radioactive parent to be considered in the calculation, i.e. $C_{p,i} = 0$ for all x and t .

$$\frac{\partial C_i}{\partial t} = \frac{\eta_i D_{pore,i}}{\eta R_i} \frac{\partial^2 C_i}{\partial x^2} - \lambda_i C_i$$

$$C_{p,i} = 0$$

$$f_{DOC} = 0$$

Eq.
4-47

Assume that at $t=0$ an amount of $N_{0,i}$ moles of nuclide i is injected at $x=0$ in an area of size A . In an infinite and homogeneous clay system, the concentration development over time will be in case of 1D diffusion:

$$C_i(x, t) = \frac{N_{0,i}}{2A\sqrt{\pi D_{app,i}t}} e^{-\frac{x^2}{4D_{app,i}t}} e^{-\lambda_i t}$$

$$D_{app,i} = \frac{\eta_i D_{pore,i}}{\eta R_i}$$

Eq.
4-48

The figure below compares the numerical solution of NRG-PA-tool in ORCHESTRA for 1D-diffusion of a flat plane source with the analytical solution. To approximate the infinite size of the clay, the NRG-PA-tool used a spatial discretization of 550 cells of 1 m thickness and a no-flow boundary at 550 m. Concentrations at 50 m distance from the source were compared.

Table 4-1 Test data for the comparison

Nuclide	$N_{0,i}$ (mole)	η_i	$D_{pore,i}$ (m^2/s)	R_i	$T_{1/2,i}$ (yrs)	η	A (m^2)
I-129	2.91E-06	1	1e-9	1	1.559E+07	1	1
Tc-99	1.56E-05	1	1e-9	5	2.110E+05		
U-235	1.06E-02	1	1e-9	300	7.042E+08		

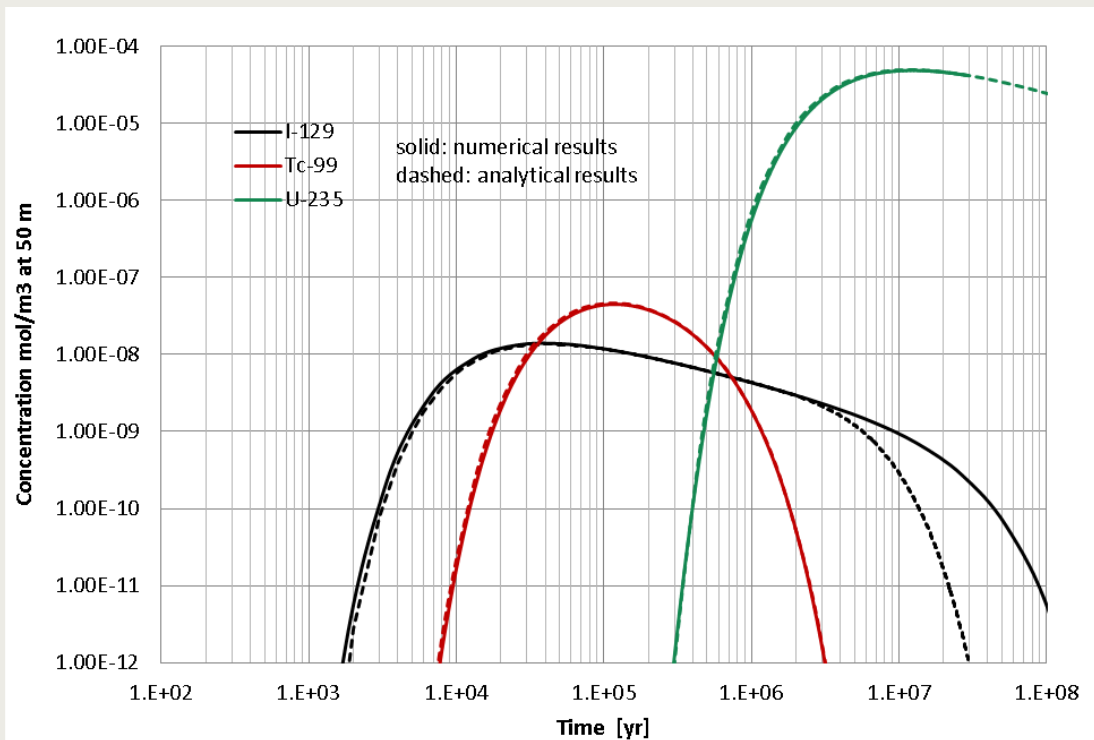


Figure 4-5 Comparison numerical and analytical results (diffusion through 50 m clay, 50 cells)

Figure 4-5 shows that the numerical results agree very well with the analytical solution. Although careful observation shows that there are small differences in initial breakthrough times, these do not affect height and time of maximum concentrations.

For I-129 the concentrations start to diverge after 3e6 years. This is caused by the fact that the analytical solution assumes an infinite medium, while the numerical model was set up to represent a "pseudo" infinite medium of 500 m clay layer on top of the initial layer of 50 m. In the numerical model the slower nuclides (Tc, U) have not reached the end of this 500 m, so their behaviour / concentrations at 50 m is not influenced by this. The faster travelling I-129 has reached the 500 m (no-flow) boundary, which explains that the I-129 concentration in the numerical model is larger than the analytical solution¹.

4.7. Solubility limit

Due to the large amount of uranium in the depleted uranium disposal section, the solubility of uranium will strongly limit the soluble concentration in the Waste-EBS compartment. As described in Section 2.3.1, the waste package and the EBS are modelled as a homogeneous mixing tank, where:

$$C(t) = \frac{A(t)}{V} = \frac{A_d(t) - A_a(t) - A_{out}(t)}{V}$$

$C(t)$ concentration of radionuclides in water at time t

V volume of the water

$A(t)$ amount of radionuclides in the water at time t

$A_d(t)$ amount of radionuclides dissolved from the waste matrix up to time t

$A_a(t)$ amount of radionuclides absorbed to EBS materials at time t

$A_{out}(t)$ amount of radionuclides that has migrated into the clay up to time t

¹ By means of multiple reflections an analytical solution can be constructed for same the geometry that was used in the NRG-PA-tool. That analytical solution is fully in line with the numerical solution, also after 3e6 years.

In case of a solubility limit, $A_d(t)$ and $A_a(t)$ precisely balance $A_{out}(t)$, such that $C(t)$ is constant and equal to the solubility limit S as long as the amount of undissolved nuclides has not been depleted.

The NRG-PA-tool can set the maximum concentration in the source compartment to S , and account for the eventual depletion of the radionuclide. Actually, the NRG-PA-tool can apply a solubility limit and the associated accounting for precipitated nuclides in each calculation cell (or finite volume).

Illustration of the impact of a solubility limit in the waste-EBS compartment

The solubility limit in the waste EBS compartment is mathematically modelled as a Dirichlet boundary condition at $x=0$:

$$C(x = 0, t) = S$$

as long as undissolved radionuclide are available in the source.

In the long run, assuming that the amount of radionuclides in the source is sufficiently large, a stationary solution can develop:

$$\frac{\partial C}{\partial t} = D_{app} \frac{\partial^2 C}{\partial x^2} = 0$$

This equation is called the Laplace equation. In case of one-dimensional diffusion, the Laplace equation has the following solution for stationary conditions, and assuming that the concentration in the aquifer is small and can be ignored in comparison with the concentration in the clay:

$$C(x, t) = S - \frac{S}{L}x$$

$C(x, t)$ stationary concentration (mol/m³) of nuclides in water
 S solubility limit (mol/m³)
 x transport distance (m)
 L thickness of the clay layer (m)

resulting in a stationary flux J :

$$J = A \left((1 - f_{DOC})\eta_i D_{pore,i} + f_{DOC}\eta_{DOC} D_{pore,DOC} \right) \frac{S}{L}$$

where:

J diffusive mass flux [mol/s] through a horizontal area A [m²].

An important observation is that the stationary flux is proportional to the size of the cross section A . A conservative result can be achieved by using the maximum cross section size, which is found at the clay-aquifer interface.

A less conservative solution can be obtained by introducing a geometry factor g_3 in the equation:

$$J = g_3 A \left((1 - f_{DOC})\eta_i D_{pore,i} + f_{DOC}\eta_{DOC} D_{pore,DOC} \right) \frac{S}{L}$$

An appropriate value of g_3 can be determined by solving the Laplace equation in 2 or 3 dimensions for the OPERA geometry. This calculation is not part of the NRG-PA-model; an appropriate value for the OPERA geometry can be pre-calculated in a separate analysis. It is expected that $0.5 < g_3 < 0.75$.

4.8. Effect of non-linear Freundlich adsorption

Although assuming linear adsorption is in most cases likely adequate when estimating the behaviour of trace elements, sometimes the adsorption behaviour deviates from linearity. We illustrate here what the effects of non-linearity would be on predicted migration rates by comparing results of a linear sorption (K_d) model with those of a non-linear Freundlich model.

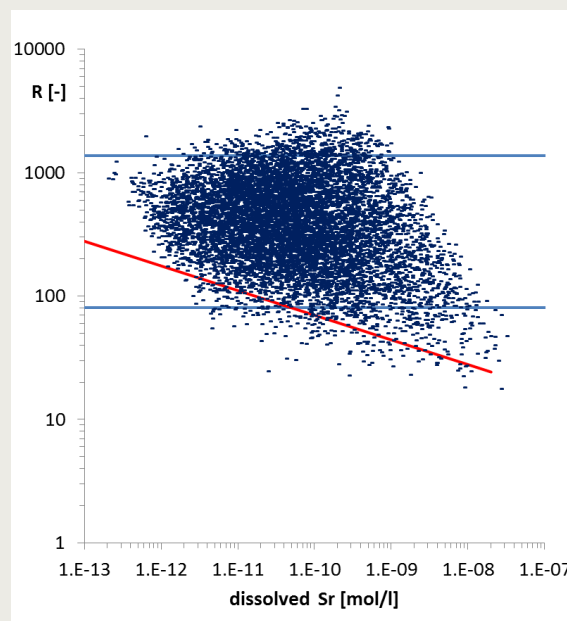


Figure 4-6 Concentration dependent Freundlich sorption (red line)

One of the strengths of ORCHESTRA is that the simple linear relation between C and n_{total} can not only be replaced by a full thermodynamic model system describing the equilibria between adsorbed and dissolved species, but also by a the non-linear Freundlich adsorption model.

The non-linear Freundlich and the linear K_d reactive transport model for Boom Clay were compared (Figure 4-7). The results show very similar concentrations at the top of the Boom Clay as a function of time. Maximum concentrations, time of breakthrough and decay rates agree very well. The main difference is the more abrupt increase in concentrations at breakthrough in case of the complex reactive model. This is caused by the fact that in the non-linear model retardation values and thus migration rates are concentration dependent. As a result, at low concentrations the retardation is stronger and therefore migration rates become slower. This causes breakthrough of low concentrations to happen later than in case of the linear model. However, because the K_d values at maximum concentrations in the linear and non-linear case are comparable, the breakthrough of maximum concentrations is unchanged.

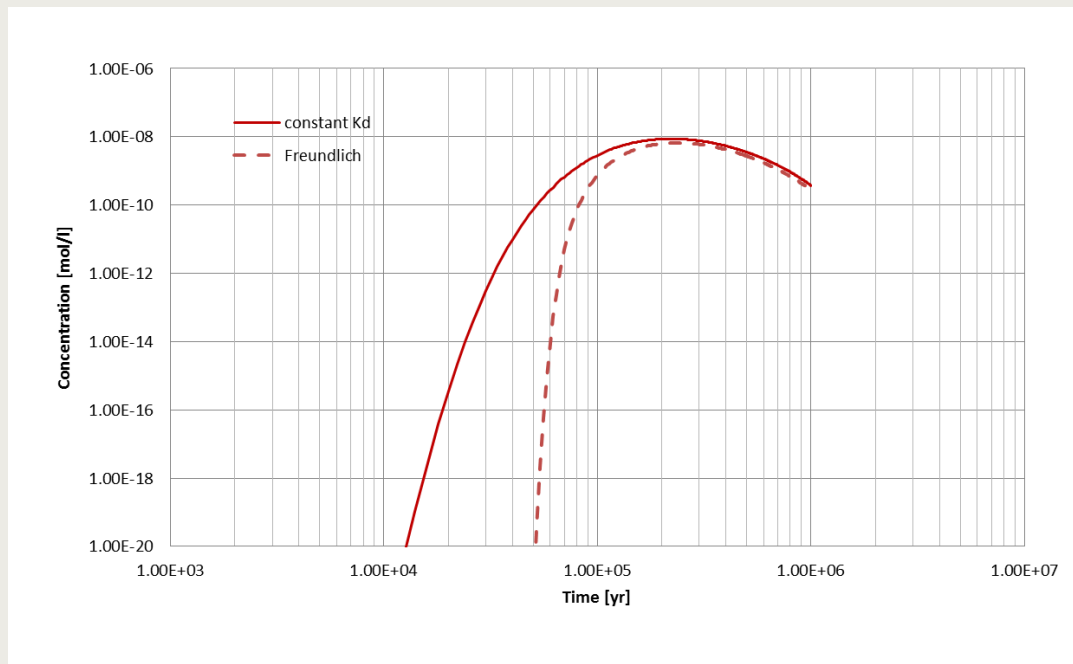


Figure 4-7 Comparison of linear and non-linear (Freundlich) sorption on reactive transport through Boom Clay

An important premise to this result is that the K_d value in the linear model was set to the low end value of the K_d scatterplot observed at the expected maximum concentration in the system. As the latter is not always known in advance, a conservative strategy for the linear adsorption model is to use a K_d value found at the lowest end of the scatter range.

4.9. Approach used in PA model

The following summarises the (mathematical) PA model for transport through clay and its implementation in the NRG-PA-tool:

- The diffusion of radionuclide through the clay layer can be modelled by a one-dimensional diffusion equation using a constant K_d model. This is also consistent with the approaches used in Belgium and France for modelling transport through the clay layer.
- K_d values can be obtained for each nuclide by measurements and/or calculations. For the OPERA research program K_d values have been calculated.
- The NRG-PA-tool uses a nuclide/species specific pore diffusion coefficient, a nuclide specific through-diffusion porosity and the total porosity for the adsorption. Differences between the through-diffusion porosity and the total porosity result in an additional retention caused by a 'dead-end' pore effect.
- A conservative strategy to account for non-linear adsorption is to use a constant K_d value found at the lowest end of the scatter range.
- The NRG-PA tool treats the simultaneous diffusion of dissolved nuclides and diffusion by DOC explicitly.
- Precipitation effects can be accounted for by using a solubility limit (in the source compartment). In this case, some attention must be given to geometrical correction for the size of the cross-section to be used in a one-dimensional approach.

5. Boom Clay model computer code, input data and parameters

This chapter describes the ORCHESTRA computer model for the calculation of the reactive transport in the compartment Boom Clay (Section 5.1), the input parameters required by this code (Section 5.2) and the output produced at the end of the calculations (Section 5.3).

5.1. The ORCHESTRA computer code

The open source reactive transport modelling framework ORCHESTRA (Meeussen, ORCHESTRA: An object-oriented framework for implementing chemical equilibrium models, 2003) was used as the main tool for the OPERA PA calculations. ORCHESTRA (Objects Representing CHEmical Speciation and TRANsport) is widely used for development of state-of-the-art mechanistic models and for applying these models for risk assessment of complex soil or cement-based systems.

Different from other programmes, the model definitions within ORCHESTRA are not build in the source code but can be defined as input at the run time making it possible to store the model definitions in a data base that can be accessed and altered by the user. There are no restrictions on the choice of the chemical models and transport equations, new models can be implemented without adjustment of the source code.

The ORCHESTRA code is accompanied by a standard object database (in text format) containing predefined model objects for chemical (e.g. complexation, adsorption, precipitation etc.) and physical (e.g. convection, diffusion) processes that can be extended and/or combined with user defined models.

In the simplified model for migration in Boom Clay, the reactive behaviour of the radionuclides was simplified to an effective retardation process by replacing the multi-surface model by an alternative version using a distribution factor K_d or retardation factor R for each nuclide.

5.2. Required input

The input required by the ORCHESTRA code for complex reactive transport through Boom Clay boils down to following key data:

- source term,
- thermodynamic data of the species in which the radionuclides are present,
- thermodynamic data of the species that have a (relevant) interaction with the species in which the radionuclides are present,
- thermodynamic properties of the Boom Clay (chemical composition of the clay water),
- a grid of cells (mixed volumes) representing the geometry of the system under consideration,
- connections between cells, including definition of process governing interaction between cells (e.g. diffusion, convection),
- content of each of the cells,
- molecular diffusion coefficients,
- radioactive decay data.

In the ORCHESTRA code for simplified reactive transport the thermodynamic data are no longer required being replaced by (a range of) distribution factors (K_d), and all other input data remaining unchanged.

Generic parameters, such as for example radio-decay data (see Figure 5-1) that are not likely to vary between different scenarios are stored in separate input file(s).

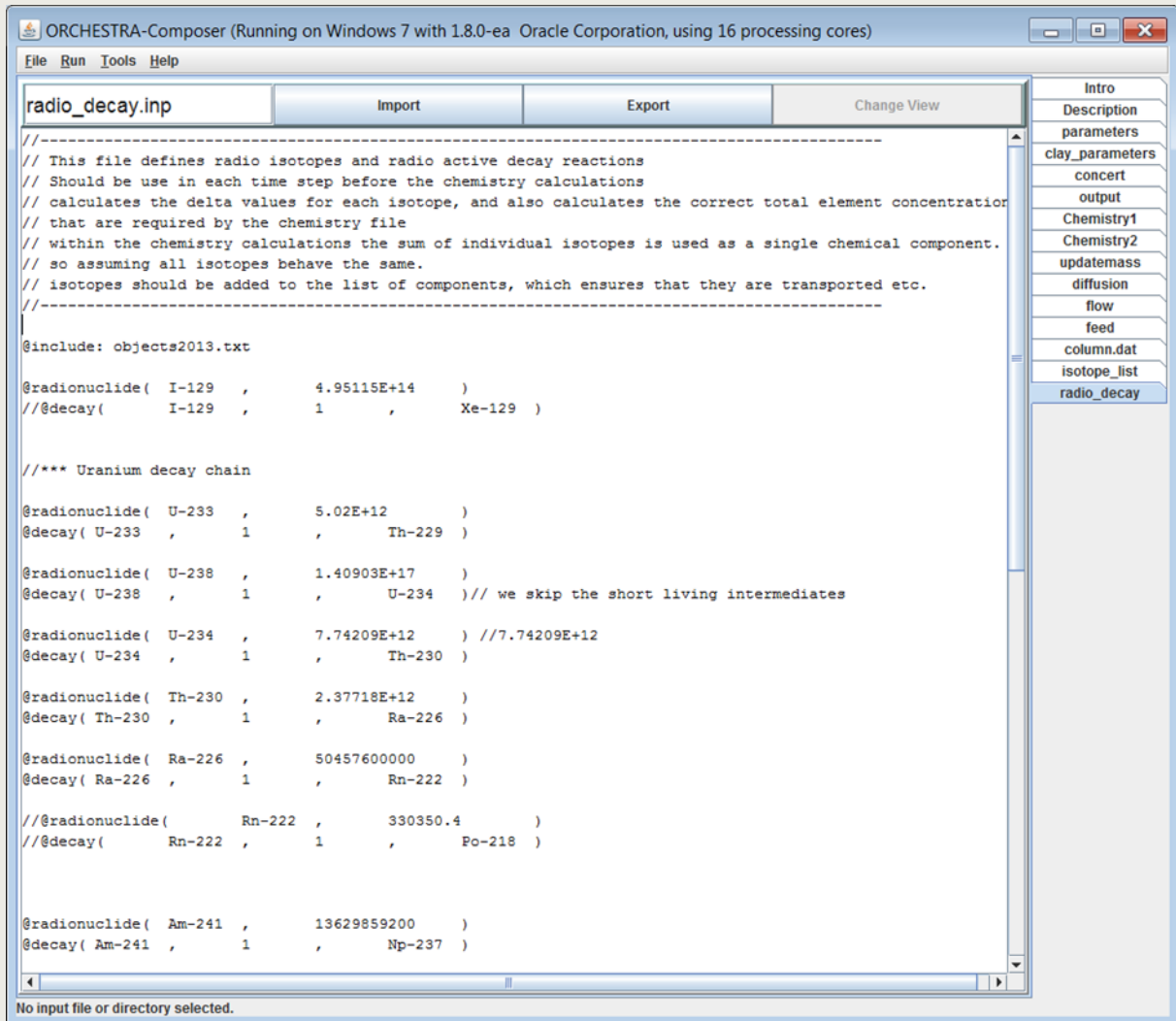


Figure 5-1 Screenshot of the input file containing radioactive decay data considered in the reactive transport model for the Boom Clay compartment

The relevant input data that define a specific input scenario will be specified within the central file parameters.txt (see Figure 5-2). This makes it easier to have a quick overview of the most important input parameters.

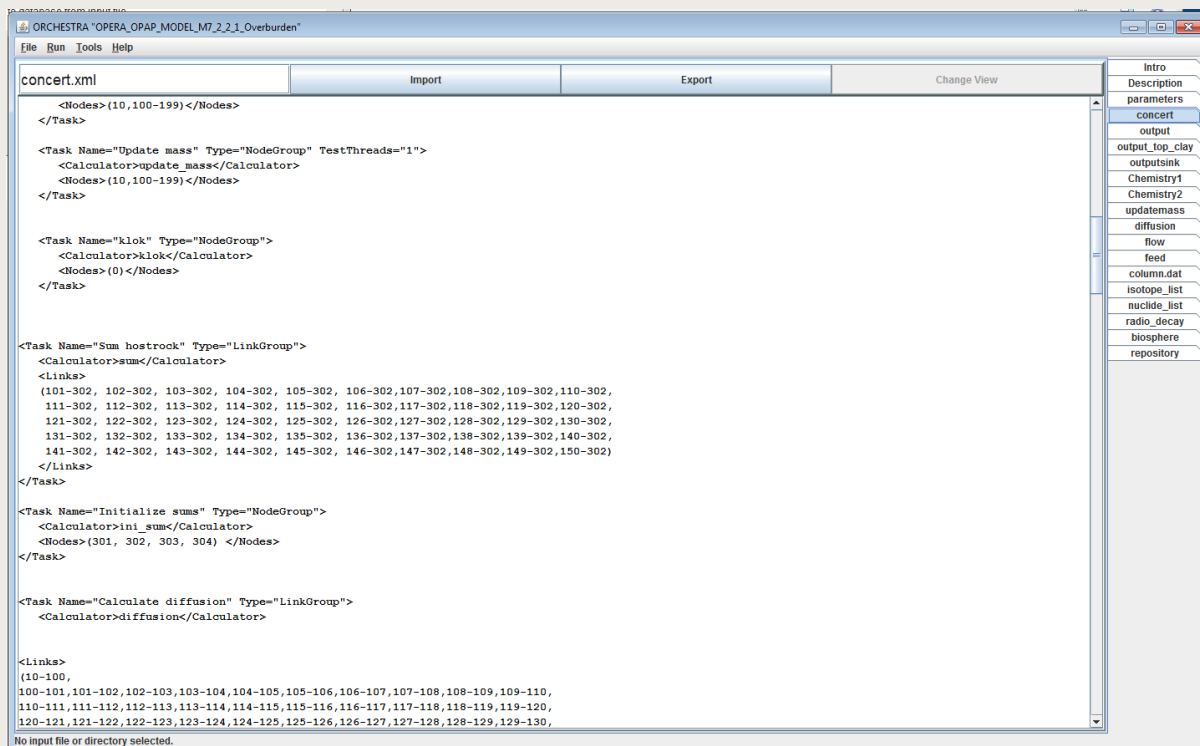


Figure 5-4 Concert.xls

5.3. Required output

The OPERA compartment models are integrated in a *PA integrated modelling environment* enabling repeated calculations of predefined scenarios. This *PA integrated modelling environment* will allow the calculation of the Safety and Performance indicators as developed in Task 7.3.1 of the OPERA Research Plan (Rosca-Bocancea & Schröder, 2013).

The indicators related to the host rock (Boom Clay) compartment have been selected from the list of indicators proposed for the OPERA Safety Case. The output from the Boom Clay model necessary for the calculation of the indicators related to the host rock compartment was established based on the calculation methodology of the indicators provided in Section 2.2 in (Schröder & Rosca-Bocancea, Safety and Performance Indicator calculation methodology, 2013) and provided for each indicator in Table 5-1.

The first four indicators (*Radiotoxicity concentration in clay water*, *Radiotoxicity in the compartment 'host rock'*, *Radiotoxicity flux from compartment 'host rock'* and *Time-integrated radiotoxicity flux from the compartment 'host rock'*) can be applied to various compartments. The next indicator (*Host rock confinement factor* is related explicitly to the host rock compartment. The *Contribution of each safety function* is a combined indicator showing the contribution of each of the performance indicators based on safety functions to the overall performance of the integrated repository system in terms of percentage, and is thus 'partially' related to the host rock compartment. The last indicator (*Retardation due to migration through host rock*) is one of the performance indicators based on safety functions and is related to the host rock compartment by definition. For purpose of internal consistency checks and for comparison reasons, it was proposed to calculate both radiotoxicity and activity-based indicators based on safety function in the OPERA safety assessment (Schröder & Rosca-Bocancea, Safety and Performance Indicator calculation methodology, 2013, p. 14).

Table 5-1 Indicators for the OPERA Safety Case related to the host rock compartment (Schröder & Rosca-Bocancea, Safety and Performance Indicator calculation methodology, 2013, p. 6)

<i>Indicator</i>	<i>Output from the host rock model necessary for the calculation of the indicator</i>
Radiotoxicity concentration in clay water	activity concentration [Bq/m ³] of radionuclide <i>n</i> in the clay water
Radiotoxicity in the compartment 'host rock'	activity [Bq] of radionuclide in compartment 'host rock'
Radiotoxicity flux from compartment 'host rock'	activity flux [Bq/yr] of radionuclide released from compartment 'host rock'
Time-integrated radiotoxicity flux from the compartment 'host rock'	activity flux [Bq/yr] of radionuclide released from compartment 'host rock'
Host rock confinement factor	activity [Bq] of radionuclide <i>n</i> in compartment 'host rock'
Contribution of each safety function	activity [Bq] of radionuclide <i>n</i> in compartment 'host rock'
Retardation due to migration through host rock	activity flux [Bq/yr] of radionuclide <i>n</i> released from compartment 'host rock'

From the table above it can be concluded that the indicators related to the host rock compartment are based on the following three key sets of data:

- activity concentration [Bq/m³] of radionuclide *n* in the clay water (in any cell of the compartment),
- total activity [Bq] of radionuclide *n* in compartment 'host rock',
- activity flux [Bq/a] of radionuclide *n* released from compartment 'host rock'.

The present version of the PA code for the host rock compartment is set up to provide concentration-based output:

- concentration [mol/m³] of radionuclide *n* in the clay water,
- total amount [mol] of radionuclide *n* in compartment 'host rock',
- flow² [mol/s] of radionuclide *n* released from compartment 'host rock'.

The concentration-based data sets can be easily and straightforwardly converted to activity based data sets and thereafter into activity and/or radiotoxicity-based indicators. This conversion is currently carried out by post processing.

Data on concentrations and fluxes can be provided for each cell (pair) of the numerical model (see example output in Figure 5-5. The total amount of radionuclides in the compartment is represented by a single set of data.

² In common language 'flux' means the quantitative description of flow, also intended in the reports on safety and performance indicators. In Computational Fluid Dynamics, however, 'flux' is a reserved term for 'flow density' while flow is surface integral of the flux; i.e. flux in (mol/s m²) and flow in (mol/s). To reduce ambiguity sometimes the terms 'flux density' and 'volume flow' are used.

ORCHESTRA-Composer (Running on Windows 7 with 1.8.0-ea Oracle Corporation, using 16 processing cores)

File Run Tools Help

output.dat	Import	Export	Change View
Var: time_years	I-129.tot	Am-241.tot	Am-243.tot
Data: 9.98858447e-1	1.00000000e-20	1.00000000e-20	1.00000000e-20
Data: 9.9887306e2	1.00000000e-20	1.04560917e-20	1.00000000e-20
Data: 1.99871575e3	1.00000000e-20	1.13476626e-20	1.00000000e-20
Data: 2.99757420e3	1.00000000e-20	1.00732301e-20	1.00000000e-20
Data: 3.99643265e3	1.00000000e-20	1.22056117e-19	1.00000000e-20
Data: 4.99529110e3	1.24967890e-19	8.72771324e-19	1.01887347e-20
Data: 5.99414954e3	8.39642809e-18	2.14777007e-18	1.18086125e-20
Data: 6.99300799e3	1.79417894e-16	3.6946377e-18	1.53584195e-20
Data: 7.99186644e3	1.80781173e-15	5.23673510e-18	2.08838027e-20
Data: 8.99072489e3	1.09436118e-14	6.63008948e-18	2.82380718e-20
Data: 9.98958333e3	4.62110025e-14	7.76804136e-18	3.71255787e-20
Data: 1.09884418e4	1.49892268e-13	8.57075368e-18	4.71394443e-20
Data: 1.19873002e4	3.98557018e-13	9.02166170e-18	5.78458065e-20
Data: 1.29861587e4	9.09036037e-13	9.15983278e-18	6.88487055e-20
Data: 1.39850171e4	1.83740412e-12	9.04952249e-18	7.98176619e-20
Data: 1.49838756e4	3.37127081e-12	8.75857358e-18	9.04939588e-20
Data: 1.59827340e4	5.71731226e-12	8.35395972e-18	1.00708290e-19
Data: 1.69815925e4	9.08696602e-12	1.26454026e-17	1.12905848e-19
Data: 1.79804509e4	1.36849070e-11	1.37154512e-17	1.24231811e-19
Data: 1.89793094e4	1.96931000e-11	1.06330391e-17	1.33125018e-19
Data: 1.99781678e4	2.72654068e-11	8.53685583e-18	1.40703524e-19
Data: 2.09770263e4	3.65215634e-11	7.18467610e-18	1.47237024e-19
Data: 2.19758847e4	4.75445348e-11	6.22465106e-18	1.52857104e-19
Data: 2.29747432e4	6.03799672e-11	5.47848110e-18	1.57650230e-19

No input file or directory selected.

Intro
Description
parameters
clay_parameters
concert
output
Chemistry1
Chemistry2
updatemass
diffusion
flow
feed
column.dat
isotope_list
radio_decay

Figure 5-5 Example of an ORCHESTRA output file

6. Benchmark ORCHESTRA vs. CLAYPOS

The alternative model used by GRS for comparison purposes is described in Section 6.1. Section 6.2 gives an overview of the adopted assumptions and parameters values for the validation calculations. The results of the CLAYPOS and ORCHESTRA calculations are presented in the Sections 6.3 and 6.4 and their comparison is carried out and discussed in Section 6.5.

The benchmark has been developed and executed in a relatively early stage of the OPERA research program. Many of the data to be used in the final calculations were under investigation at that time in the research program. Therefore data from older research programs (CORR, PAMINA) have been used to set up a test calculation for this benchmark. These test data, which are now classified as "arbitrary test data", are expected to be at best of the same order of magnitude as the eventual data used for the OPERA PA calculations.

6.1. Benchmarking code

The alternative model used by GRS for comparison purposes is based on the model used in the generic German clay study TONI (Rübel, Becker, & Fein, 2007) and adapted to the Dutch situation.

The release of radionuclides from the near field has been calculated by the computer code CLAYPOS (Rübel, Becker, & Fein, 2007). The results of the calculations are time-dependent values of flows and concentrations of all considered radionuclides at the intersection of the clay to the overburden (gsk file of CLAYPOS). These data are part of the input to the code POSA which was applied later in Task 7.2.2 to calculate advective transport in the aquifer (geosphere).

The code CLAYPOS is part of the RepoTREND package [Reiche et al., 2011] developed by GRS. CLAYPOS calculates one-dimensional transport of contaminants in the liquid phase of a porous medium, taking retardation (K_d concept) and radioactive decay into account.

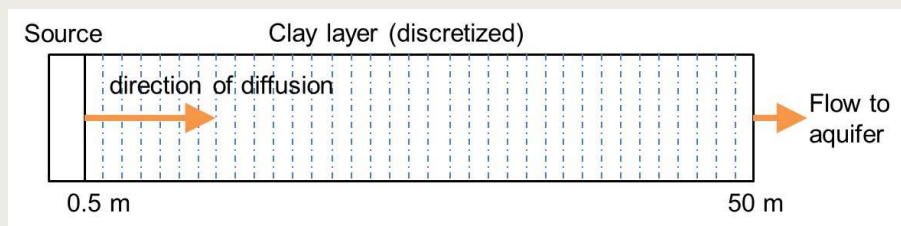


Figure 6-1 Transport path in the CLAYPOS model for Boom Clay

The transport of radionuclides starts at the source. At the beginning all radionuclides are within the source and are released from the waste matrix over time according to the mobilization rate. An almost instantaneous release can be assumed by a high mobilization rate. This fast release yields the initial concentrations of all radionuclides in the source, which are given by inventory and solubility limits.

The transport in the Boom Clay is by diffusion taking a planar geometry into account, see (Rübel, Becker, & Fein, 2007) for details. The transport path has been divided into 190 elements of 0.26 m length. A variant has been calculated with 50 elements of 1 m length to be consistent to the ORCHESTRA discretization; there were only minor differences in the resulting concentrations and fluxes.

6.2. Benchmark case

The total amount of nuclides in the inventory (Table 6-1) is assumed to dissolve completely at the start of the simulation ($t = 0$ years) in the specified representative volume element (see Figure 6-1). This is realised in the CLAYPOS calculations by a high mobilisation rate (1000 yr^{-1}) and high solubilities of all elements. The idea behind this model is to calculate the release of radionuclides from the entire repository and the assumption, that all of these radionuclides are transported to the same place in the aquifer (overburden).

As pointed out in Section 2.3.1, for the numerical calculation the volume and shape of the EBS can be chosen freely. A cross section of $260\,000 \text{ m}^2$ has been chosen, and a height of 1 m in CLAYPOS and 2 m in ORCHESTRA. Since the EBS/clay system is mirror-symmetrical in the horizontal centre-plane through the EBS, for the calculations only the upper part is considered: the thickness of the EBS in the upper part is 0.5 m (CLAYPOS) or 1 m (ORCHESTRA). The chosen test value for the porosity is 0.15. No retardation of the respective nuclides in the material matrix of the source cell was considered. The dissolved radionuclides come immediately into contact with the overlying clay layer (see Figure 6-1), so diffusion towards the clay layer starts at the beginning of the simulation (at $t = 0 \text{ yr}$).

The first 11 radionuclides in Table 6-1 represent activation and fission products. The rest of radionuclides represent the actinide decay chains. These decay chains consist of a larger number of isotopes than presented in the table. For transport calculations in a safety assessment however, the number of isotopes for which the activity must be calculated by the computer code, can be limited to the longer lived ones, as the short lived nuclides will be in equilibrium with their parents. The following simplified decay chains have been included in the PA model for migration in clay:

4N chain: Cm-248 -> Pu-244 -> Pu 240 -> U-236 -> Th-232

4N+1 chain: Cm-245 -> Am-241 -> Np-237 -> U-233 -> Th-229

4N+2 chain: Cm-246 -> Pu-242 -> U-238 -> U-234 -> Th-230 -> Ra-226

4N+3 chain: Cm-247 -> Am-243 -> Pu-239 -> U-235 -> Pa-231

Table 6-1 Arbitrary test values for initial inventory and half-lives of radionuclides used in the benchmark calculations

<i>Radionuclide</i>	<i>Inventory [mol]</i>	<i>Half-life ORCHESTRA [yr]</i>	<i>Half-life CLAYPOS [yr]</i>
C-14	9.51E+00	5.70E+03	5.73E+03
Cl-36	4.12E-01	3.01E+05	3.00E+05
Ca-41	2.66E-01	1.40E+05	1.03E+05
Ni-59	2.68E+03	7.60E+04	7.50E+04
Se-79	1.47E+01	1.10E+06 ³	1.10E+06
Mo-93	2.20E+00	4.00E+03	3.50E+03
Zr-93	7.67E+03	1.53E+06	1.50E+06
Tc-99	1.27E+04	2.14E+05	2.10E+05
Pd-107	2.09E+03	6.50E+06	6.50E+06
Sn-126	1.80E+02	1.00E+05	2.35E+05
I-129	2.79E+02	1.61E+07	1.57E+07
Ra-226	1.14E-01	1.60E+03	1.60E+03
Th-229	1.81E-05	7.34E+03	7.88E+03

³ The half-life of Se-79 is under debate since several years (Songsheng, et al., 1997). The actual value of $3.77\text{E}+05 \text{ yr}$ (Hart, 2015) should be taken into account in future calculations.

<i>Radionuclide</i>	<i>Inventory [mol]</i>	<i>Half-life ORCHESTRA [yr]</i>	<i>Half-life CLAYPOS [yr]</i>
Th-230	1.40E+00	7.54E+04	7.54E+04
Pa-231	1.52E-01	3.28E+04	3.28E+04
Th-232	6.58E+05	1.41E+10	1.41E+10
U-233	5.06E-03	1.59E+05	1.59E+05
U-234	4.59E+03	2.46E+05	2.46E+05
U-235	1.44E+06	7.04E+08	7.04E+08
U-236	1.22E+03	2.37E+07	2.34E+07
Np-237	2.47E+03	2.14E+06	2.14E+06
U-238	3.56E+08	4.47E+09	4.47E+09
Pu-239	4.20E+02	2.41E+04	2.41E+04
Pu-240	2.31E+02	6.56E+03	6.56E+03
Am-241	1.97E+03	4.33E+02	4.32E+02
Pu-242	2.59E+01	3.74E+05	3.75E+05
Am-243	6.23E+02	7.36E+03	7.37E+03
Pu-244	8.44E-04	8.00E+07	8.00E+07
Cm-245	8.09E+00	8.50E+03	8.50E+03
Cm-246	2.13E-03	4.73E+03	4.73E+03
Cm-247	3.88E-05	1.56E+07	1.56E+07
Cm-248	5.20E-06	3.39E+05	3.40E+05

The radionuclides Se-79, Tc-99, I-129, Np-237, U-238 were chosen for benchmarking as well as the members of the 4N-decay chain: Cm-248 -> Pu-244 -> Pu 240 -> U-236 -> Th-232.

Table 6-2 and Table 6-3 give all the data of the transport path in clay as used in the present calculation. The boundary condition for these near-field calculations (which yields an almost zero concentration boundary condition for diffusive flow out of the Boom Clay) is determined by the volume flow rate in the overburden.

Table 6-2 Arbitrary test values for the compartments waste and host rock (Boom Clay) radionuclides used in the benchmark calculations

<i>Parameter</i>	<i>Dimensions</i>	<i>Compartment</i>	
		<i>Waste</i>	<i>Host rock</i>
(half) height (L)	m	0.5 - 1	50
porosity (ϵ)	-	0.15	0.15
solid density (ρ_s)	kg/m ³	2600	2600
cross section (A)	m ²	260,000	260,000
effective diffusion coefficient* (D_e)	m ² /s	2.0E-10	2.0E-10
concentration in the aquifer	mol/m ³	$\approx 0^{**}$	$\approx 0^{**}$

* Combination of molecular D in pore water and tortuosity

** Very small - value depends on the flow of water through the aquifer

Table 6-3 Arbitrary test values for nuclide specific transport parameters for Boom Clay radionuclides used in the benchmark calculations

<i>Radionuclide</i>	<i>Retardation factor R [-]</i>	<i>Distribution coefficient K_d [m³/kg]</i>
I, Se, Cm	1	1.00E-06
Am	1000	6.78E-02

Radionuclide	Retardation factor R [-]	Distribution coefficient K_d [m ³ /kg]
Np	1000	6.78E-02
Pa	400	2.71E-02
Pu	1000	6.78E-02
Ra	50	3.30E-03
Tc	5	2.70E-04
Th	500	3.38E-02
U	300	2.03E-02

6.3. Results of CLAYPOS calculations

Time dependent concentrations of the selected radionuclides calculated with CLAYPOS at the end of the transport path in the clay layer are given in Figure 6-2. The calculations are for 50 cells with 1 m length each.

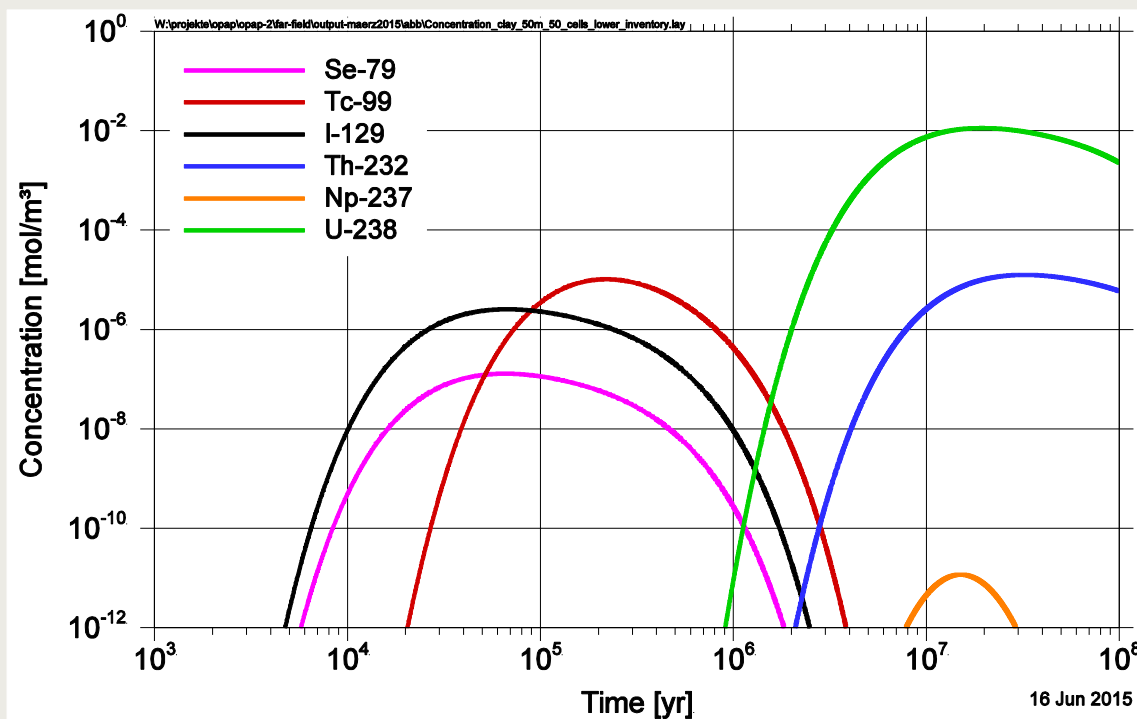


Figure 6-2 Time dependent CLAYPOS concentrations at the end of the transport path in Boom Clay (distance in clay 49.5 m)

The effect of retardation is obvious. The concentration maxima of the non retarded nuclides Se-79 and I-129 appear before 100.000 years, while the low retarded nuclide Tc-99 has a maximum after 200,000 years. The strongly retarded nuclides Th-232, Np-237 and U-238 show maximum concentrations not earlier than 10⁷ years.

Figure 6-3 shows the temporal evolution of the concentrations for different radionuclides along the transport path. The diffusion-controlled decrease of the concentrations can be seen; at the end of the transport path (49.5 m) the more pronounced decrease is caused by the zero-boundary condition at the intersection to the overburden.

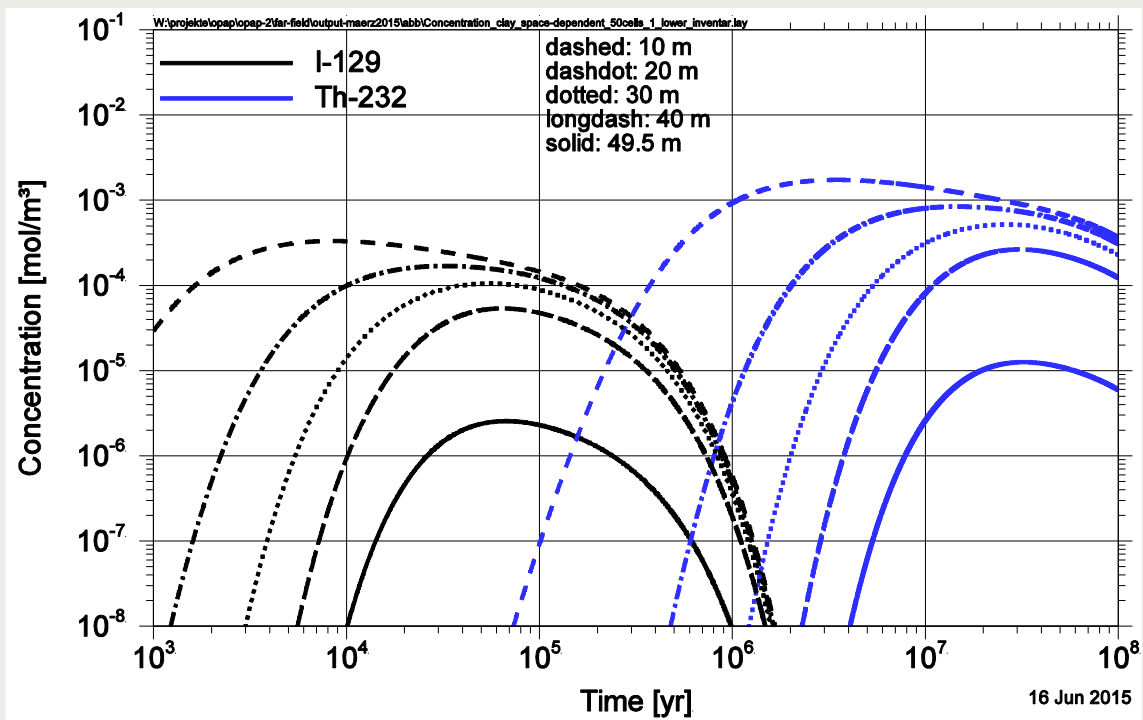
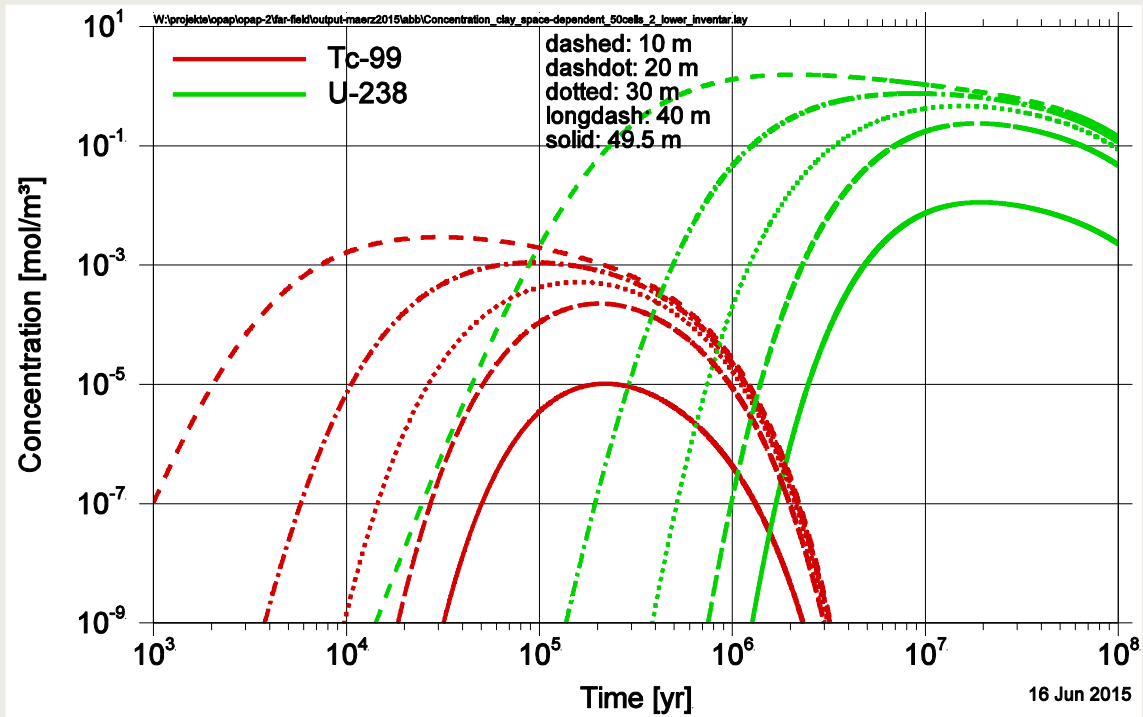


Figure 6-3 Temporal evolution of CLAYPOS concentrations along the transport path in Boom Clay for selected radionuclides

In Figure 6-4 the nuclide flow rates from clay to aquifer calculated with CLAYPOS are presented. The effect of retardation can be seen by a similar time shift in the flow rate maxima (e. g. maxima of U-238 and Th-232 are much later than I-129 and Se-79) compared to the concentration maxima in Figure 6-2.

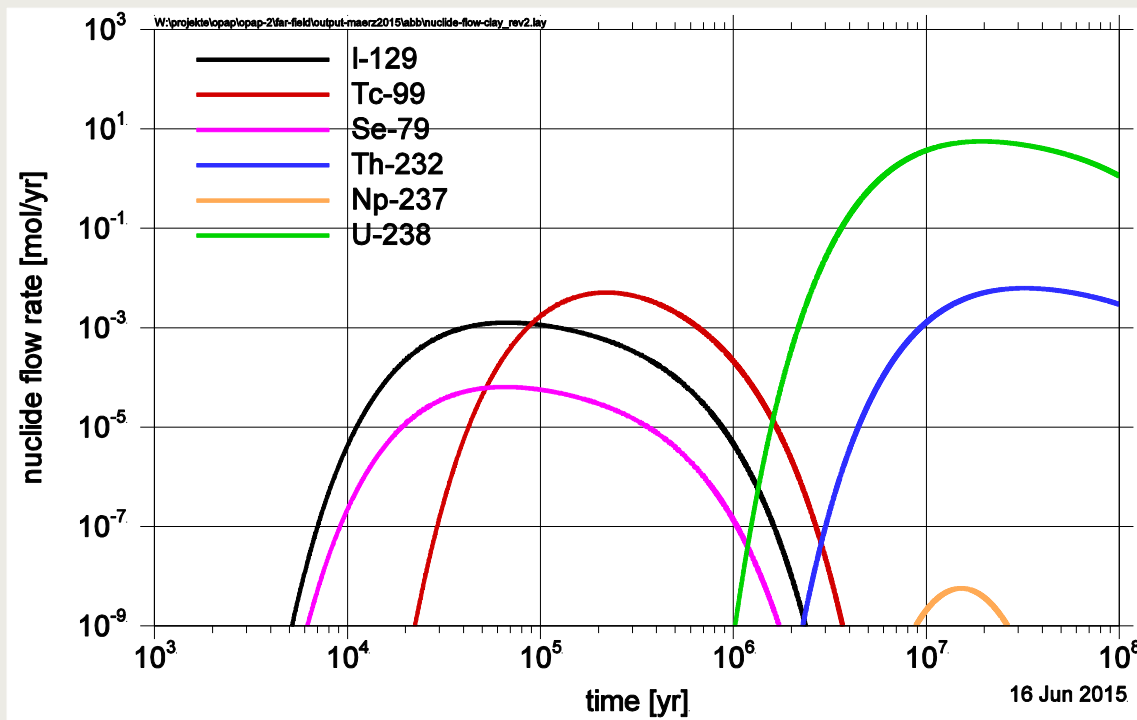


Figure 6-4 Nuclide flow rate at the clay/aquifer interface as calculated by CLAYPOS

6.4. Results of ORCHESTRA calculations

The present version of the PA model for host rock provides as output the following three concentration-based sets of data for each of the radionuclides considered in the Performance Assessment (see Section 5.3 for more detail):

- concentration [mol/m³] of radionuclide n in the clay water,
- total amount [mol] of radionuclide n in compartment 'host rock',
- flow [mol/s] of radionuclide n released from compartment 'host rock'.

Data on concentrations and fluxes can be provided for each cell (pair) of the numerical model. The total amount of radionuclides in the compartment is represented by a single set of data.

For the presentation of the ORCHESTRA results similar figures as for CLAYPOS (see chapter 6.3) are shown. As the curves are almost identical to the CLAYPOS curves, a detailed discussion of the results is omitted here. Some figures demonstrating the comparison are shown in Chapter 6.5.

The time dependent concentrations of the selected radionuclide concentrations calculated with ORCHESTRA for the end of the transport path are shown in Figure 6-5. The performance indicator *Radiotoxicity concentration in the host rock compartment* is obtained by converting these concentration-based concentrations to radiotoxicity based concentrations.

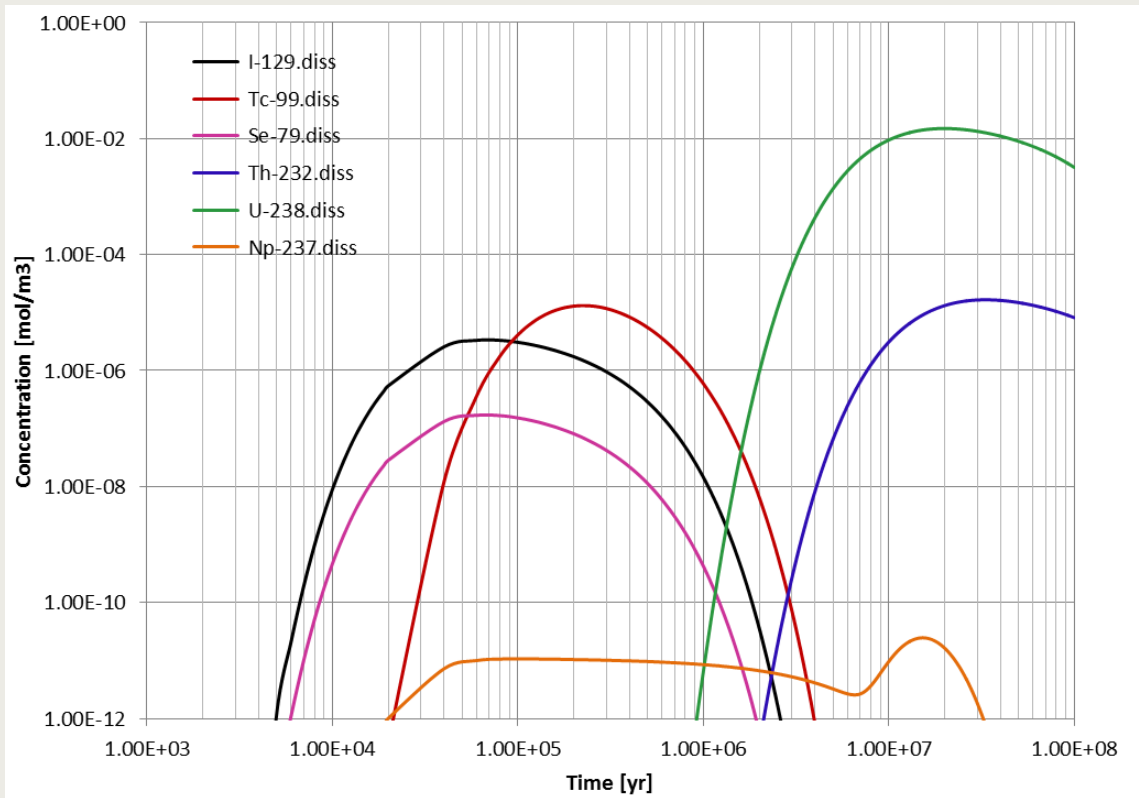
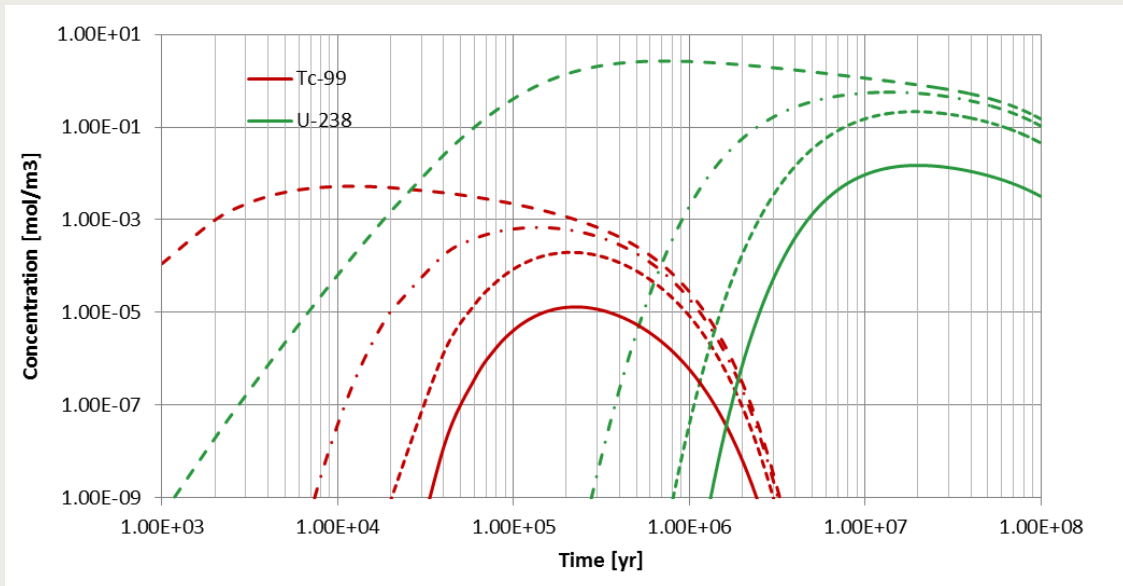


Figure 6-5 Time dependent ORCHESTRA concentrations at the end of the transport path in Boom Clay (distance in clay 49.5 m)

When combined on the same graph, the concentrations at selected positions along the transport path give a good representation of the retardation and delay function of the host rock (see Figure 6-6).



a)

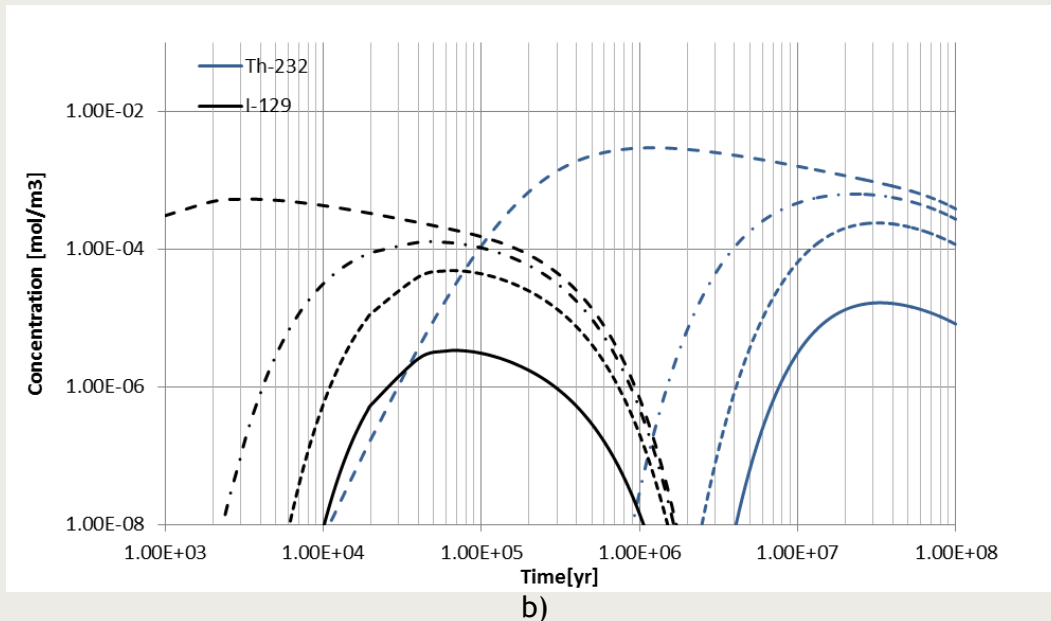


Figure 6-6 Time evolution of ORCHESTRA concentrations along the transport path (at 5, 25, 40, 49.5 m) in Boom Clay for selected radionuclides (Tc-99, U-238, Th-232, I-129)

Figure 6-7 represents the evolution in time of the total amount of nine radionuclides in the Boom Clay compartment.

When converted to radiotoxicity, these data represent the indicator *Radiotoxicity in the compartment 'host rock'*. In combination with radiotoxicities in other compartments these data permit the graphical representation of the indicator *Contribution of each safety function*. The integration of the total radiotoxicities in time produces the *Time-integrated radiotoxicity flux from the compartment 'host rock'* indicator. The indicator *Host rock confinement factor* can be calculated by dividing the radiotoxicity in the Boom Clay compartment by the total disposed radiotoxicity.

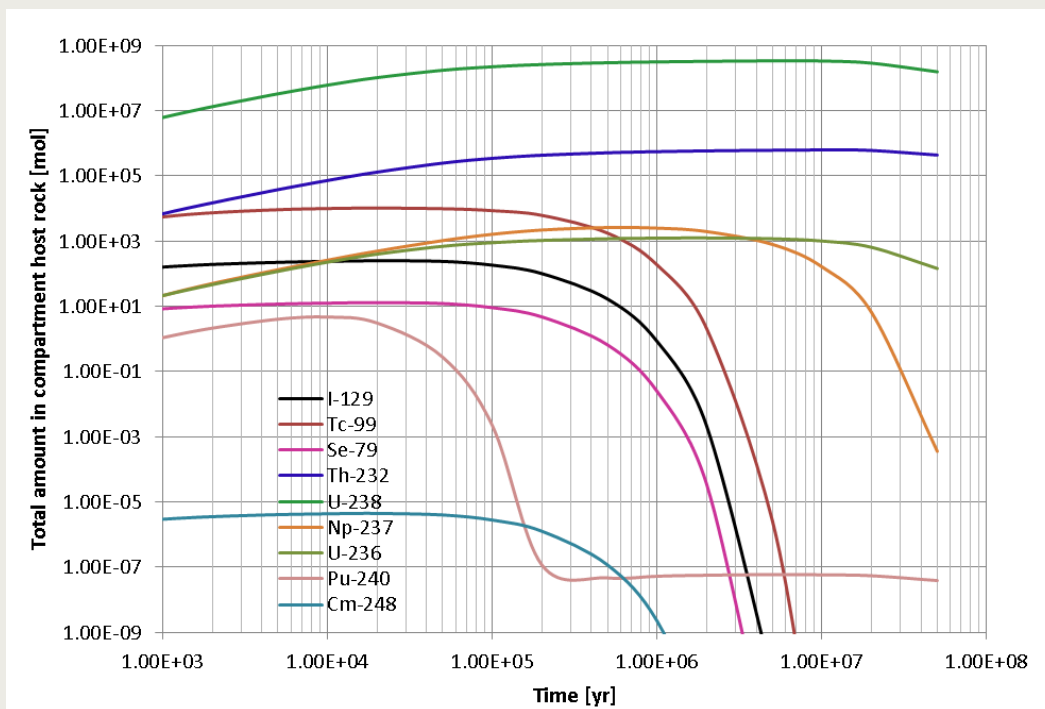


Figure 6-7 Total amount of selected radionuclides in the host rock compartment

The third set of output data - the temporal evolution of the radionuclide fluxes across the boundary clay/aquifer (see Figure 6-8) - form the base of the rest of the indicators related to Boom Clay compartment. The calculations are carried out for a time frame of 1E+8 years. The maxima of all the concentration curves are met within this time frame.

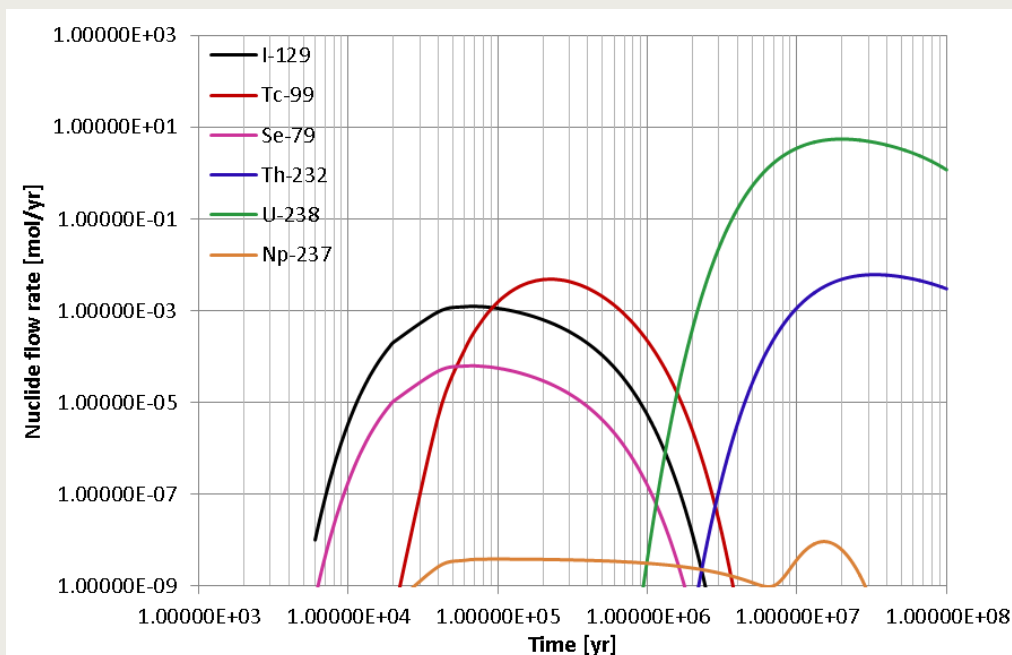


Figure 6-8 Nuclide flow rate at the clay/aquifer interface calculated by ORCHESTRA

When converted to radiotoxicity, these data represent the indicator *Radiotoxicity flux from the compartment 'host rock'* and the integration in time of the radiotoxicity flux represents the indicator *Time-integrated radiotoxicity flux from the compartment host rock*.

The *Retardation due to migration through buffer and host formation* can be calculated by dividing the time integrated radiotoxicity flux released by the time-integrated (up to time t) radiotoxicity flux released from waste package.

6.5. Comparison CLAYPOS and ORCHESTRA results

It was chosen to compare two sets of data: concentrations and fluxes out of the compartment. These two sets of data form the base for the calculation of all other necessary data sets and give a good indication of the correct implementation of the mathematical model for the Boom Clay compartment.

For comparison purpose, the time evolution of these two quantities is presented graphically and the maximum concentrations and fluxes as well as the time step of the maxima were tabulated. To be able to compare the breakthrough and the maximum reached concentrations and fluxes of the strong retarded radionuclides a simulation period of 100 million years was chosen.

The comparison of the time dependent CLAYPOS and ORCHESTRA concentrations at the end of the transport path in the overburden is given in Figure 6-9 below.

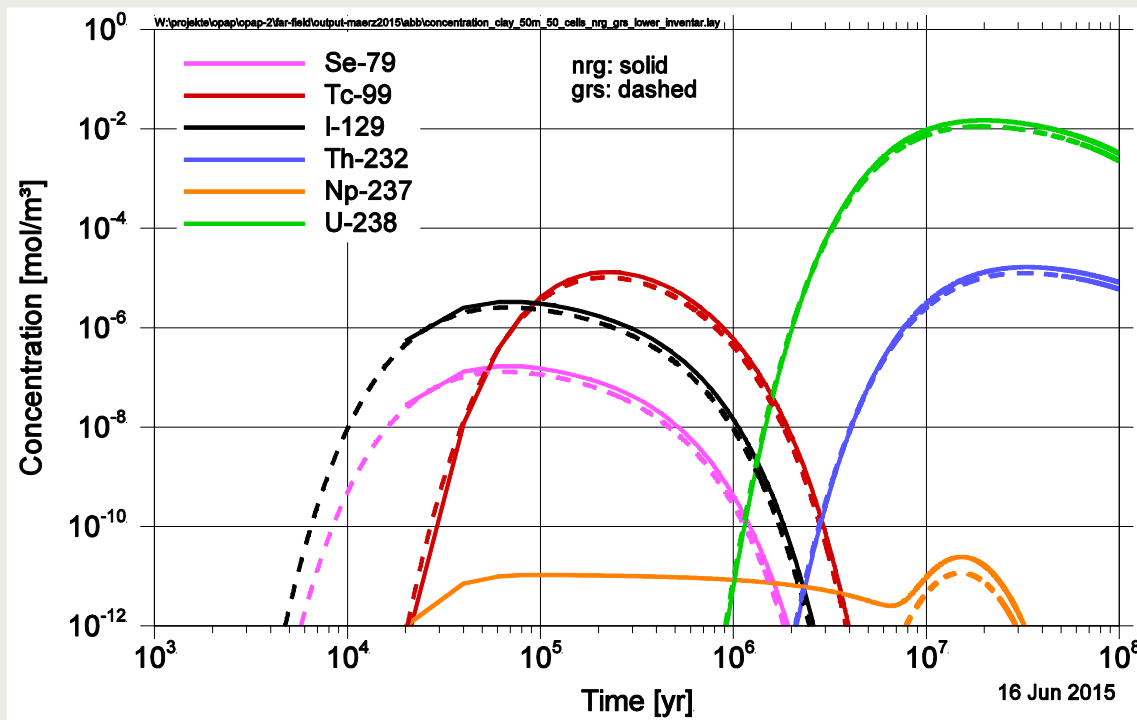


Figure 6-9 Time dependent ORCHESTRA and CLAYPOS concentrations at the end of the transport path in the clay layer (49.5 m)

The concentration maxima at the top of the host rock and the related time points calculated by ORCHESTRA PA model for Boom Clay and by CLAYPOS are summarized in Table 6-4.

Table 6-4 Concentration maxima at the top of the host rock and time of their occurrence

Radionuclide	ORCHESTRA		CLAYPOS	
	Maximum dissolved concentration [mol/m ³]	Time points of maximum concentration [y]	Maximum dissolved concentration [mol/m ³]	Time points of maximum concentration [y]
Se-79	1.69E-07	5.99E+04	1.29E-07	6.52E+04
Tc-99	1.32E-05	2.20E+05	1.03E-05	2.19E+05
I-129	3.33E-06	7.99E+04	2.56E-06	6.73E+04
Th-232*	1.66E-05	3.32E+07	1.26E-05	3.17E+07
U-236*	3.67E-08	1.52E+07	2.37E-08	1.49E+07
Np-237	2.46E-11	1.51E+07	1.77E-11	1.50E+07
U-238	1.50E-02	1.99E+07	1.13E-02	1.94E+07
Pu-240*	5.32E-19	5.13E+07	4.96E-15	4.99E+07
Cm-248*	5.52E-14	5.99E+04	4.19E-14	6.16E+04

*Members of the decay chain 4N: Cm-248 -> Pu-244 -> Pu 240 -> Th-232

Figure 6-10 shows the calculated flow rates of selected radionuclides at the intersection from the clay layer to the aquifer.

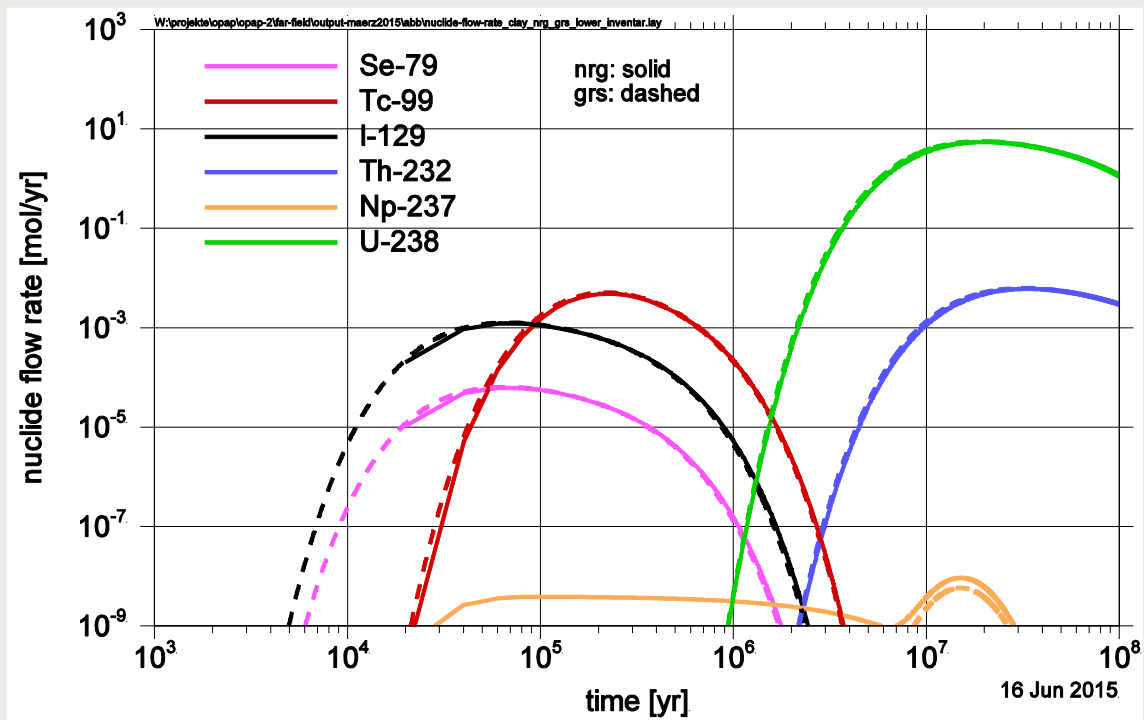


Figure 6-10 Nuclide flow rates at the clay/aquifer interface calculated by ORCHESTRA and CLAYPOS

The flow rate maxima and the related time points calculated by the ORCHESTRA PA model for Boom Clay and by CLAYPOS are given in Table 6-5 below.

Table 6-5 Flow rate maxima and time of their occurrence

Radionuclide	ORCHESTRA		CLAYPOS	
	Maximum flow rate [mol/yr]	Time points of maximum flow rate [y]	Maximum flow rate [mol/yr]	Time points of maximum flow rate [y]
Se-79	6.20E-05	5.99E+04	6.45E-05	6.56E+04
Tc-99	4.87E-03	2.20E+05	5.13E-03	2.19E+05
I-129	1.22E-03	5.99E+04	1.27E-03	6.72E+04
Th-232*	6.09E-03	3.32E+07	6.27E-03	3.22E+07
U-236*	1.34E-05	1.53E+07	1.18E-05	1.50E+07
Np-237	9.33E-09	1.51E+07	5.85E-09	1.51E+07
U-238	5.48E+00	1.99E+07	5.63E+00	1.94E+07
Pu-240*	1.95E-16	5.11E+07	2.47E-12	5.02E+07
Cm-248*	2.02E-11	5.99E+04	2.09E-11	6.21E+04

*Members of the decay chain 4N: Cm-248 -> Pu-244 -> Pu 240 -> Th-232

The CLAYPOS and ORCHESTRA results on most of the radionuclides concentrations in the compartment water (Figure 6-9, Table 6-4) show generally a good agreement. The difference is caused by the parameterization of the concentration boundary condition at the interface, which is slightly different in CLAYPOS and ORCHESTRA. This leads to relatively large differences in the concentrations near the interface.

The CLAYPOS and ORCHESTRA results on radionuclide fluxes from the host rock compartment into the geosphere (Figure 6-10, Table 6-5) show a good agreement within the analyzed time range and hereby prove the correct implementation of the numerical model in the ORCHESTRA code for reactive transport through the Boom Clay compartment.

It also shows that the slightly different parameterization of the concentration boundary condition in the clay-aquifer interface has a negligible impact on the nuclide flow rates.

Differences in the values of Pu-240 and Np-237 have been recognized to be caused by a numerical inconsistency in CLAYPOS. This will be resolved in the next version of CLAYPOS.

7. Conclusions and recommendations

The PA model for clay has been treated:

- 1) on a conceptual level, explaining which processes govern the migration in clay,
- 2) on a mathematical level,
- 3) on the numerical level, as an implementation in ORCHESTRA.

The conceptual description describes how the PA model for the clay compartment fits in the total PA model, and explains why diffusion is the main transport process in the clay compartment. The clay properties that determine the transport and the adsorption in the clay have been discussed qualitatively.

The mathematical model is described, as well as the premises for correct use of the model. An extension to the commonly used model is described and implemented: the PA model treats the simultaneous diffusion of dissolved nuclides and diffusion by DOC explicitly.

The numerical implementation of the PA model in ORCHESTRA has been described, including a benchmark with the German ClayPos code, and an outlook into more advanced options of ORCHESTRA are described (in particular the use of a non-linear sorption model).

It is concluded that, in particular because there is actual little data on the Boom clay in the Netherlands, and the clay properties are location (i.e. site) dependent, the constant K_d model and its implementation in the form of the NRG-PA-tool in ORCHESTRA is adequate for the generic safety assessment performed in OPERA.

8. References

- Groot, T. d., Berg, M. v., Dijke, J. v., Janssen, J., & Veldkamp, A. (1993). *Evaluation of salt bodies and their overburden in The Netherland for the disposal of radioactive waste, part d., Fluvial and subglacial erosion*. Haarlem: Rijks Geologische Dienst.
- Grupa, J. (2014). *Report on the safety assessment methodology*. OPERA-PU-NRG2121.
- Grupa, J., Hart, J., & Wildenborg, T. (2017). *Description of relevant scenarios for the OPERA disposal concept*. OPERA-PU-NRG7111.
- Hart, J. (2015). *Determination of the inventory Part A: Radionuclides*. OPERA-PU-NRG1112A.
- Jansen, S., & Griffioen, J. (2014). *Autonomous geochemical development of the Boom Clay: Literature review and modelling*. draft OPERA-PU-521TNO-3.
- Koenen, M., & Griffioen, J. (2014). *Mineralogical and geochemical characterization of the Boom Clay in the Netherlands*. OPERA-PU-TNO521-1.
- LLNL. (1999, March). Methane Hydrate: A Surprising Compound. *S&TR*, pp. 20-22.
- Meeussen, J. (2003). ORCHESTRA: An object-oriented framework for implementing chemical equilibrium models. *Environ. Sci. Technol.* 37, (6), 1175-1182.
- Meeussen, J., Rosca-Bocancea, E., Schröder, T., Koenen, M., Valega Mackenzie, F., Maes, N., et al. (2017). *Model representation of radionuclide diffusion in Boom Clay*. OPERA-PU-NRG6131.
- ONDRAF/NIRAS. (2001). *SAFIR 2 - Safety Assessment and Feasibility Interim Report 2*. NIROND 2001-06 E.
- ONDRAF/NIRAS. (2013). *Research, Development and Demonstration (RD&D) Plan, state of the art report as of December 2012*. NIROND-TR-2013-12 E.
- Rosca-Bocancea, E., & Schröder, T. (2013). *Development of Safety and Performance Indicators*. OPERA-PU-NRG7311.
- Rübel, A., Becker, D.-A., & Fein, E. (2007). *Radionuclide transport modelling—Performance assessment of repositories in clays*. GRS-228, GRS mbH.
- Schröder, T., & Meeussen, J. (2017). *Final report on radionuclide sorption in Boom Clay*. OPERA-PU-NRG6123.
- Schröder, T., & Meeussen, J. (2017). *Reference database with sorption properties*. OPERA-PU-NRG6122.
- Schröder, T., & Rosca-Bocancea, E. (2013). *Safety and Performance Indicator calculation methodology*. OPERA-PU-NRG7312.
- Shackelford, C., & Moore, S. (2013). Fickian diffusion of radionuclides for engineered containment barriers: Diffusion coefficients, porosities, and complicating issues. *Engineering Geology* 152, 133-147.
- Songsheng, J., Jingru, G., Shan, J., Chunsheng, L., Anzhi, C., Ming, H., et al. (1997). Determination of the half-life of ⁷⁹Se with the accelerator mass spectroscopy technique. *Nuclear Instruments and Methods in Physics Research B* 123, 405-409.
- Valstar, J., & Goorden, N. (2016). *Hydrological transport in the rock formations surrounding the host rock*. OPERA-PU-DLT621.
- Veen, J. t., & Dario, V. (2015). *Future evolution of the geological and geohydrological properties of the geosphere*. OPERA-PU-TNO412.
- Verhoef, E., & Schröder, T. (2011). *Research Plan*. OPERA-PG-COV004.
- Verhoef, E., Neeft, E., Grupa, J., & Poley, A. (2011). *Outline of a disposal concept in clay*. OPERA-PG-COV008.
- Verweij, H., Nelskamp, S., Valstar, J., & Govaerts, J. (2016). *Definition of the future boundary conditions for the near-field model*. OPERA-PU-TNO421_2.
- Vis, G.-J., & Verweij, J. (2014). *Geological and geohydrological characterization of the Boom Clay and its overburden*. OPERA-PU-TNO411.
- Wildenborg, A., Orlic, B., Lange, G. d., Leeuw, C. d., Zijl, W., Weert, F. v., et al. (2000). *Transport of Radionuclides disposed of in Clay of Tertiary Origin (TRACTOR)*. Utrecht: TNO-report NITG 00-223-B.

Appendix 1 Diffusion accessible porosity

The surface of the Boom clay minerals, under in situ conditions, a dissociation of the S-OH groups occurs, resulting in the creation of negative charges at these mineral surfaces. This characteristic leads to is an electrostatic repulsion of the anions (Donnan exclusion) and sorption of the cations. The diffusion accessible porosity of the non-sorbing anions such as iodide will therefore be less than that of the cations and neutral species such as tritiated water or dissolved silica (Si(OH)₄).

(Shackelford & Moore, 2013) give a concise treatment of various definitions of porosity and diffusion coefficients for porous media. Fick's first law for one-dimensional diffusion in porous media commonly is written as one of the following:

$$\frac{J}{A} = -\eta_{i,da} G D_{aq} \frac{dC}{dx} = -\eta_{i,da} D^* \frac{dC}{dx} = -D_e \frac{dC}{dx} = -\eta_i D_{pore} \frac{dC}{dx} \quad \text{Eq. A-1}$$

where, following (Shackelford & Moore, 2013):

J	diffusive mass flux (mol/s) through a horizontal area A (m ²),
$\eta_{i,da}$	diffusion accessible porosity [1],
G	geometry factor accounting for the pore structure (i.e. tortuosity, constrictivity),
D_{aq}	diffusion coefficient or diffusivity of the solute in free water or 'free-solution' diffusion coefficient (in absence of porous medium) (m ² /s),
D^*	effective diffusion coefficient (m ² /s)
D_e	also is known as the effective diffusion coefficient (m ² /s) (geological sciences literature)
η_i	effective or through-diffusion porosity [1],
D_p	pore diffusion coefficient (m ² /s)
C	aqueous phase concentration of the solute (mol/m ³),
x	distance in the direction of transport (m).

In this report the diffusion equation was derived under the assumption that the migrating species can access the pore volume that is determined by the porosity η . Using the terminology of (Shackelford & Moore, 2013) this porosity should be termed the diffusion accessible porosity $\eta_{i,da}$. Eq. 4-14 should be rewritten as:

$$\frac{\partial C_i}{\partial t} = \frac{\eta_i}{\eta_{i,da}} \frac{D_{pore,i}}{R_i} \frac{\partial^2 C_i}{\partial x^2} - \lambda_i C_i + \lambda_{p,i} \frac{\eta_i}{\eta_{i,da}} \frac{\eta_{p,i,da}}{\eta_{p,i}} \frac{R_{p,i}}{R_i} C_{p,i} \quad \text{Eq. A-2}$$

So the apparent diffusion coefficients reads:

$$D_{app} = \frac{\eta_i}{\eta_{i,da}} \frac{D_{pore,i}}{R} = \frac{D^*}{R} \quad \text{Eq. A-3}$$

If $\eta_i < \eta_{i,da}$, a fraction of the pore volume ($\eta_{i,da} - \eta_i$) consists of dead end pores. In case of concentration changes, also the species in the dead-end pores have to migrate, which slows down the concentration change. This shows in the value of D_{app} .

If the definitions of (Shackelford & Moore, 2013) are compared with the equations in (ONDRAF/NIRAS, 2001), differences show:

$$\frac{J}{A} = -\eta_{i,da} G D_{aq} \frac{dC}{dx} = -\eta_{i,da} D_{pore} \frac{dC}{dx}$$

$$D_{app} = \frac{D_{aq}}{RR_f} = \frac{GD_{aq}}{R} = \frac{D_{pore}}{R}$$

(ONDRAF/NIRAS,
2001, p.
11.3.8.2.1)

Therefore D_{pore} in (ONDRAF/NIRAS, 2001) can be read as D^* in (Shackelford & Moore, 2013). Alternatively, it could be that for Boom clay $\eta_{i,da} = \eta_i$, in that case $D^* = D_{pore}$, and the two terminologies are consistent. However, the latter is unlikely as discussed in the next paragraph.

(Shackelford & Moore, 2013) report that for most mudrocks and similar porous media $\eta_{i,da} \approx \eta_i$, however fractured rock, highly compacted bentonite buffers and smectitic based geologic formations may show considerable amount of dead-end pores in the form of immobile liquid fraction ("bound water") in the interparticle and interlayer pore spaces within each clay particle. Boom clay contains a considerable amount of smectites (10% - 20%), therefore it must be expected that for Boom clay $\eta_i < \eta_{i,da}$.

Another complication occurs when considering the relation between the retardation coefficient R and the distribution coefficient K_d . In general this relation is:

$$R = 1 + \frac{K_d \rho_{dry}}{\eta}$$

Eq. A-4

The retention is coupled to the distribution coefficient by the mass of the clay material. Since adsorption occurs at the grain-liquid interfaces, the adsorption is actually proportional to the size of these internal surfaces. In Eq. A-4 it is assumed implicitly that the mass and the internal surface are proportional.

In case a K_d is determined in a batch experiment or by a calculation, all internal surfaces may be accessible for adsorption (due to the way the batch experiment is performed or the assumptions for the calculation). However, for in situ conditions not all internal surfaces may be accessible, especially in the case of anions and DOC's, where $\eta_{i,da} < \eta_{total}$.

In the case that K_d is determined in a test volume of clay where η_{total} is accessible, but in situ $\eta_{i,da} < \eta_{total}$, K_d should be defined as:

$$n_{i,adsorbed} = K_d M_{acc} C_i$$

Eq. A-5

where M_{acc} is the diffusion accessible mass, which is equal to or less than the solid mass M_s in a small test volume, depending on $\eta_{i,da}$ and η_{total} .

In a first approach it can be assumed that the relation between M_{acc} and M_s in a given volume of clay relates to the diffusion accessible volume of water (V_{acc}) and the total volume of pore water (V_p) in the same volume of clay, and subsequently to $\eta_{i,da}$ (diffusion accessible porosity) and η_{total} (total porosity) as follows:

$$\frac{M_{acc}}{M_s} = \frac{V_{acc}}{V_p} = \frac{\eta_{i,da} V}{\eta_{total} V} = \frac{\eta_{i,da}}{\eta_{total}}$$

Eq. A-6

So:

$$B_{total,i} = \frac{K_d \eta_i M_s}{V \eta_{total}} C_i + C_i \eta_{i,da} = \frac{K_d \rho_{dry} \eta_{i,da} V}{V \eta_{total}} C_i + C_i \eta_{i,da} = \eta_i \left(1 + \frac{K_d \rho_{dry}}{\eta_{total}} \right) C_i \quad \text{Eq. A-7}$$

This will eventually lead to:

$$R = 1 + \frac{K_d \rho_{dry}}{\eta_{total}} \quad \text{Eq. A-8}$$

where:

η_{total} is the accessible porosity that was used for the determination of K_d .

This seems in contradiction with (ONDRAF/NIRAS, 2001, p. 11.3.8.4.5), eq. (9), where:

$$R = 1 + \frac{K_d \rho_{dry}}{\eta_{i,da}} \quad \text{(ONDRAF/NIRAS, 2001, p. 11.3.8.4.5),}$$

However, (ONDRAF/NIRAS, 2001, p. 11.3.8.2.3) says: As regards the anions for which a sorption process is observed (by ligand exchange), a diffusion accessible porosity of 0.30 is postulated for use at the Mol site, i.e. $\eta_{i,da} = 0.3 = \eta_{total}$.

Appendix 2 Advection diffusion equation

In some altered evolution scenarios, a combination of unusual high hydraulic gradients and/or a decrease of the net permeability of the clay layer may cause advective transport to play a role.

The fluid flow can be described by Darcy's law:

$$\bar{J}_{fluid} = \frac{AK}{L\mu} \nabla p$$

where:

- J_{fluid} volume of a fluid flowing through cross-section A in the porous medium perpendicular to ∇p per unit of time (m^3/s)
- A cross-section A perpendicular to ∇p (m^2)
- L length of the porous medium (m)
- K intrinsic permeability of the porous medium (m^2)
- μ dynamic viscosity of the fluid (m^2)
- ∇p pressure gradient (excluding gravity effects) (Pa/m)

The velocity (v) of the fluid in the porous medium can be written as (now including gravity):

$$\bar{v} = \frac{\bar{u}}{\eta} = \frac{1K}{\eta\mu} (\rho\bar{g} - \nabla p)$$

where:

- v velocity (vector) of the fluid in the porous medium (m/s)
- u velocity (vector) of the fluid when extruded from the porous medium (m/s)
- g gravitation vector (m/s^2)

Consider a volume V bounded by its surface S inside the porous medium. The flux of nuclides through ds , a small part of the surface S, is:

$$j_{nuclide\ i} = -\eta_i ds D_{pore,i}(\bar{n}, \nabla C_i) + \eta_i ds(\bar{n}, \bar{v}C_i)$$

where:

- $j_{nuclide}$ nuclide flow, amount of nuclides leaving volume V through surface element ds (mol/s)
- η_i effective or through-diffusion porosity [-]
- $D_{pore,i}$ pore diffusion coefficient [m^2/s]
- \bar{n} (vector) surface normal of surface ds pointing out of volume V
- $(\bar{n}, \nabla C_i)$ scalar product of \bar{n} and the concentration gradient ∇C_i of nuclide i (mol/m^4) at the centre of ds
- $(\bar{n}, \bar{v}C_i)$ scalar product of \bar{n} and the local advective transport speed $\bar{v}C_i$ of nuclide i (mol/m^2s) at the centre of ds

Taking into account the decay and potential ingrowth of nuclides inside the volume V, the mass balance for volume V can be written as follows:

$$\iiint_V \left(\frac{\partial B_{i,total}}{\partial t} + \lambda_i B_{i,total} - \lambda_{p,i} B_{p,i,total} \right) dv = - \iint_S \left(-\eta_i D_{pore,i}(\bar{n}, \nabla C_i) + \eta_i (\bar{n}, \bar{v}C_i) \right) ds$$

The surface integral in the right hand term can be rewritten to a volume integral using the divergence theorem, also known as Gauss's theorem:

$$\iint_S \left(-\eta_i D_{pore,i} (\bar{n}, \nabla C_i) + \eta_i (\bar{n}, \bar{v} C_i) \right) ds = \iiint_V \text{div}(-\eta_i D_{pore,i} \nabla C_i + \eta_i \bar{v} C_i) dv$$

Since the volume V can be chosen arbitrarily, the following must hold:

$$\frac{\partial B_{i,total}}{\partial t} + \lambda_i B_{i,total} - \lambda_{p,i} B_{p,i,total} = -\text{div}(-\eta_i D_{pore,i} \nabla C_i + \eta_i \bar{v} C_i)$$

Reordering the terms, and rewriting $\text{div}(\nabla C_i)$ as ΔC_i , where Δ is de Laplace operator, the general diffusion advection relation with decay and ingrowth is found:

$$\frac{\partial B_{i,total}}{\partial t} = \eta_i D_{pore,i} \Delta C_i - \eta_i \text{div}(\bar{v} C_i) - \lambda_i B_{i,total} + \lambda_{p,i} B_{p,i,total}$$

If the reactive transport can be characterised by linear adsorption, as in Section 4.3, the reactive transport equation can be written as:

$$\frac{\partial C_i}{\partial t} = \frac{\eta_i}{\eta_{i,da}} \frac{D_{pore,i}}{R_i} \Delta C_i - \frac{\eta_i}{\eta_{i,da}} \frac{1}{R_i} \text{div}(\bar{v} C_i) - \lambda_i C_i + \lambda_{p,i} \frac{\eta_i}{\eta_{i,da}} \frac{\eta_{p,i,da}}{\eta_{p,i}} \frac{R_{p,i}}{R_i} C_{p,i}$$

Note, that if the X-axis is directed upwards, and the water flow \bar{v} is constant and directed upwards with magnitude v, and the concentration gradients in Y- and Z-direction are zero, the equation reduces to its one-dimensional form:

$$\frac{\partial B_{i,total}}{\partial t} = \eta_i D_{pore,i} \frac{\partial^2 C_i}{\partial x^2} - \eta_i v \frac{\partial C_i}{\partial x} - \lambda_i B_{i,total} + \lambda_{i,p} B_{p,i,total}$$

Appendix 3 Diffusive versus advective transport

The Péclet's number provides a good indication of the hydraulic regime in the engineered structures of the repository by showing the ratio between the characteristic times of diffusion and advection and has been used by ONDRAF/NIRAS, 2001 (Section 11.3.8.2.1) and ANDRA to determine the transport regime in the engineered structures of the repository. because the approaches by ONDRAF/NIRAS and ANDRA are mathematically equal, we choose to follow [ANDRA, 2005, p.194]:

$$P_e = \frac{T_d}{T_a} = \frac{L^2 \eta / D_e}{L \eta / K \nabla H} = \frac{LK ||\partial p / \partial z| - pg|}{D_e \rho g} = \frac{Lk ||\partial p / \partial z| - pg|}{D_e \mu}$$

with:

P_e	Péclet's number,
T_d	characteristic migration time by diffusion [s],
T_c	characteristic migration time by advection [s],
L	migration distance [m],
η	total porosity in the Boom Clay [-],
D_e	effective diffusion coefficient in the clay [m ² /s],
K	hydraulic conductivity of the clay [m/s],
k	intrinsic permeability of the clay [m ²],
ρ	density of the fluid [kg/m ³],
g	acceleration due to gravity [m/s ²],
μ	dynamic viscosity of the fluid [kg/(m·s)]
∇H	gradient of the hydraulic head [m/m] over the clay layer,
$ \partial p / \partial z - pg $	vertical pressure gradient [Pa/m].

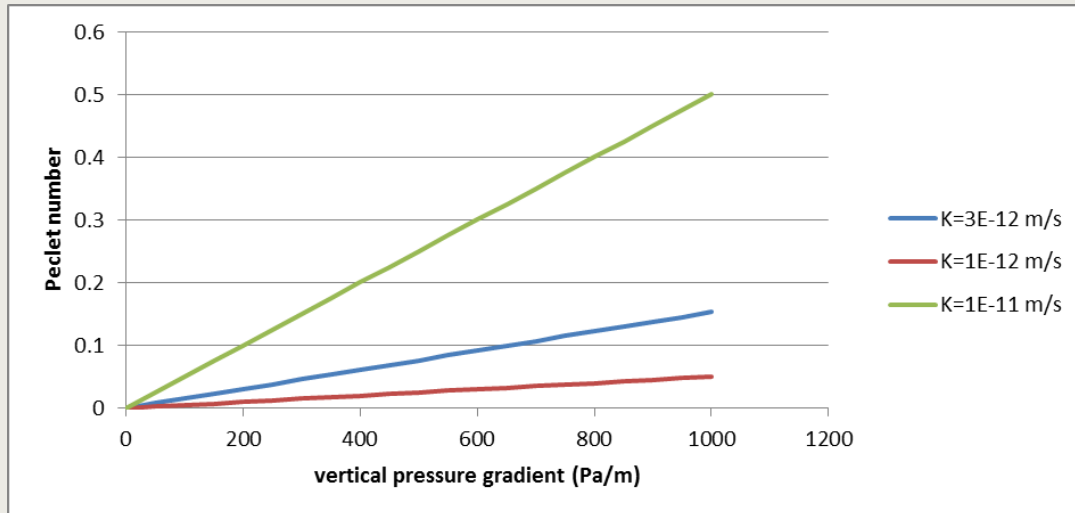
At low values of Péclet's number (less than one) the hydraulic regime is dominated by diffusion.

Table A-1 Representative parameter values for calculating the Péclet number

<i>Parameter</i>	<i>Value B*</i>	<i>Value NL</i>
L migration distance [m]	50	50
D_e effective diffusion coefficient in clay [m ² /s]	1E-10	1E-10
K permeability of the clay [m/s]	3E-12	1E-12 to 1E-11
$ \partial p / \partial z - pg $ pressure gradient [Pa/m]	2 -200	200
k intrinsic permeability of the clay [m ²]	-	1E-19 to 1E-18
ρ density of the fluid [kg/m ³]	1000	
g acceleration due to gravity [m/s ²]	9.81	
μ dynamic viscosity of the fluid [Pa·s]	-	1E-3

*[ONDRAF / NIRAS 2013, p.93 and p.135]

The figure below shows that even for high permeability and pressure gradients, the Péclet number is always less than one.



FigureA-8-1Péclet number for the Boom Clay for a conservative range of pressure gradients

References Appendix 1

[ANDRA, 2005] ANDRA, *Dossier 2005 Granite, Safety analysis of a geological repository*, ANDRA, 2005.

[ONDRAF/NIRAS, 2012] ONDRAF / NIRAS Research, *Development and Demonstration (RD&D) Plan*, state of the art report as of December 2012, NIROND-TR-2013-12 E December 2013.

Disclaimer

This report has been prepared at the request and for the sole use of the Client and for the intended purposes as stated in the agreement between the Client and Contractors under which this work was completed.

Contractors have exercised due and customary care in preparing this report, but have not, save as specifically stated, independently verified all information provided by the Client and others. No warranty, expressed or implied is made in relation to the preparation of the report or the contents of this report. Therefore, Contractors are not liable for any damages and/or losses resulting from errors, omissions or misrepresentations of the report.

Any recommendations, opinions and/or findings stated in this report are based on circumstances and facts as received from the Client before the performance of the work by Contractors and/or as they existed at the time Contractors performed the work. Any changes in such circumstances and facts upon which this report is based may adversely affect any recommendations, opinions or findings contained in this report. Contractors have not sought to update the information contained in this report from the time Contractors performed the work.

The Client can only rely on or rights can be derived from the final version of the report; a draft of the report does not bind or obligate Contractors in any way. A third party cannot derive rights from this report and Contractors shall in no event be liable for any use of (the information stated in) this report by third parties.

OPERA

Meer informatie:

Postadres
Postbus 202
4380 AE Vlissingen

T 0113-616 666
F 0113-616 650
E info@covra.nl

www.covra.nl

